

1 **Towards large-scale application of nanoporous materials in membranes for**  
2 **separation of energy-relevant gas mixtures**

3

4 Roberto Castro-Muñoz<sup>a,b\*</sup>, Kumar V. Agrawal<sup>c\*</sup>, Zhiping Lai<sup>d\*</sup>, Joaquín Coronas<sup>e,f\*</sup>

5

6 (a) Tecnológico de Monterrey, Campus Toluca, Avenida Eduardo Monroy  
7 Cárdenas 2000 San Antonio Buenavista, 50110 Toluca de Lerdo, México

8 (b) Gdansk University of Technology, Faculty of Civil and Environmental  
9 Engineering, Department of Sanitary Engineering, 11/12 Narutowicza St.,  
10 80-233, Gdansk, Poland

11 (c) Institute of Chemical Sciences and Engineering (ISIC), École  
12 Polytechnique Fédérale de Lausanne, Sion, Switzerland

13 (d) Advanced Membrane and Porous Materials Center, King Abdullah  
14 University of Science and Technology, Thuwal, 23955-6900, Kingdom of  
15 Saudi Arabia

16 (e) Instituto de Nanociencia y Materiales de Aragón (INMA), CSIC-  
17 Universidad de Zaragoza, Zaragoza 50018, Spain.

18 (f) Chemical and Environmental Engineering Department, Universidad de  
19 Zaragoza, Zaragoza 50018, Spain

20

21 **Abstract**

22 **Membranes containing** nanoporous materials (such as zeolites, metal-organic  
23 materials and 2D materials such as graphene derivatives) may allow more  
24 efficient separation of gas mixtures relevant to emerging energy technologies.  
25 For example, such membranes could be applied in the separation of gases

26 containing mixtures of carbon dioxide (CO<sub>2</sub>) and hydrogen (H<sub>2</sub>). However, these  
27 membranes are currently at a relatively low technology readiness level. Hence,  
28 here we review the opportunities and challenges of applying these porous  
29 materials in practice and at scale in membranes for possible commercialization.  
30 Besides, we highlight the necessity of improvements in the porosity control of 2D  
31 materials and the decrease in the selective membrane skin layer when adapted  
32 in asymmetric membranes. In this latter point, we declare the main limitation of  
33 porous supports, as well as the further developments in the gutter layer and  
34 supports. Additionally, we review the main membrane module configurations and  
35 process requirements, declaring the most suitable configurations (e.g. spiral  
36 wound and hollow fiber modules) at scale with promising future for highly  
37 intensified membrane modules for applicability in CO<sub>2</sub> and H<sub>2</sub> separations.  
38 Finally, apart from the conclusions derived from this review, we outline key  
39 recommendations for the researchers in the field.

40

41 **Keywords:** Gas separation; porous materials; membrane modules; hollow fibers;  
42 challenges; hydrogen separation; CO<sub>2</sub> separation.

43

#### 44 1. Introduction

45 As the world seeks to move to greener energy technologies and to lower carbon  
46 footprints and emissions, a number of gas separation processes may become  
47 more important. For example, gas mixtures related to energy production include  
48 CO<sub>2</sub>/N<sub>2</sub> (post-combustion carbon capture), CO<sub>2</sub>/CH<sub>4</sub> (production of biomethane)  
49 and H<sub>2</sub>/CO<sub>2</sub> (pre-combustion carbon capture). Current gas separation technology  
50 largely relies on thermally-driven processes, such as distillation, absorption and

51 adsorption. Yet, there is evidence that some membrane-based separations  
52 applying concentration and pressure gradients may be more energetically  
53 efficient and environment-friendly than existing processes, and they could limit  
54 carbon dioxide emissions and reduce costs [1].

55

56 High-performance membranes for gas separation consist of a composite  
57 structure in which, ideally, an ultrathin film based on selective materials is placed  
58 on top of a mechanically robust porous support, constituting a thin-film composite  
59 (TFC) membrane (see **Fig. 1**) [2]. As of now, gas separation membranes are  
60 dominated by polymeric materials due to the fact that polymers can be rapidly  
61 processed into the TFC morphology. However, the gas separation performance  
62 from the polymeric membranes is limited by the intrinsic properties of the polymer  
63 determining gas sorption and diffusion, molecular solubility, the free volume  
64 between the polymeric chains, and chain stiffness [3–5]. Some of these  
65 properties have been improved with the so-called next-generation polymeric  
66 materials, e.g., polymers with intrinsic microporosity and thermally rearranged  
67 polymers. However, the free volume in the nanoporous polymer tends to reduce  
68 as a function of time which negatively impacts the gas permeance [6,7].

69

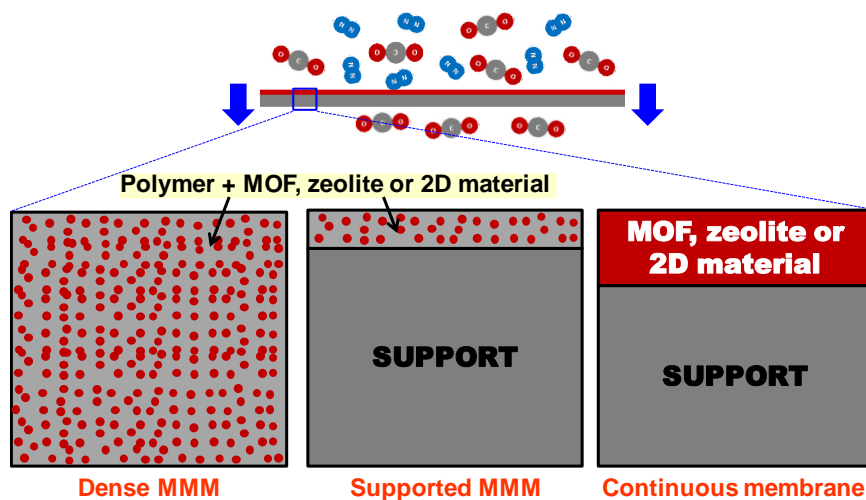
70 To improve the performance of gas separation membranes, nanoporous  
71 inorganic materials (e.g., zeolites, metal-organic frameworks or MOFs, and  
72 nanoporous two-dimensional materials) have been extensively investigated [8–  
73 11]. These materials with high porosity and thermal, chemical and mechanical  
74 robustness but mainly with pores in the range of sizes of common gas molecules  
75 can carry out molecular separations based on the relative size difference and



76 adsorption affinity [12]. Besides their implementation as TFC membranes where  
77 a thin polycrystalline film acts as a selective layer, these materials can also be  
78 used as selective fillers for a target application, constituting the so-called mixed  
79 matrix membranes (MMMs), or when prepared as a thin film on a proper porous  
80 support, thin film nanocomposite membranes (TFN)[13]. These filler-polymer  
81 combinations could overcome the main limitations of the existing membrane  
82 technologies [14]: permeance-selectivity trade-off still far from commercial  
83 applicability, membrane reliability and long-term realistic operation. However,  
84 most of the reviews published, which timely report the current state of the art of  
85 membranes for gas separation, lack in revealing the drawbacks and challenges  
86 in the commercialization of membranes containing nanofillers (mainly zeolites,  
87 MOFs and 2D materials) for possible application at the industrial scale for H<sub>2</sub> and  
88 CO<sub>2</sub> separation. Therefore, this review examines the contribution of nanoporous  
89 materials to constitute membranes for the separation of energy-relevant gas  
90 mixtures. The main families of such materials are presented together with the  
91 limitations and possible improvements of the current membrane systems  
92 regarding their implementation in large-scale and more practical applications.  
93 Additionally, we declare the membrane requirements, membrane module  
94 configurations and the most suggested configuration (like hollow fibers) for these  
95 gas separation applications, giving an overview of the hybrid membrane concepts  
96 adapted in hollow fibers for the separation of CO<sub>2</sub> and H<sub>2</sub>-containing mixtures.

97





98

99 **Fig. 1.** Scheme of the different types of gas separation membranes involving  
 100 nanoporous materials. The dense or supported (also known as TFC membranes)  
 101 polymeric membranes can be MMMs (or TFN membranes) incorporating  
 102 nanoporous fillers such as MOFs, zeolites, or others.

103

## 104 **2. Zeolites and MOFs as main components of gas separation membranes**

### 105 *2.1. Opportunities of zeolites/MOFs for gas separation*

106 Zeolites and MOFs are crystalline microporous materials, which in principle,  
 107 provide a straightforward strategy to overcome the trade-off limit of polymeric  
 108 membranes. That is, the uniform pore size offers precise molecular sieving to  
 109 achieve high selectivity, while the highly porous structure allows fast transport of  
 110 the smaller molecules to achieve high flux. If the pore size is adequately selected,  
 111 zeolite/MOF membranes can differentiate molecules at a size difference of 0.02  
 112 nm or less [15]. Such clear-cut molecular sieving implies that almost every  
 113 important pair of the gas system can be effectively separated.

114

115 The pore size of zeolite/MOF membranes is mainly determined by the framework  
116 structure. It can also be fine-tuned through ion exchange and surface modification  
117 [16]. The hybrid inorganic/organic MOF structures are much more diverse and  
118 easier for surface modification. Furthermore, the permanent porosity and the rigid  
119 framework structure can avoid the undesirable aging and plasticization effects  
120 observed for polymers [6]. Compared to MOF membranes, zeolite membranes  
121 are more stable in high temperatures, more resistant to organic solvents, and  
122 more robust in harsh conditions, providing unique opportunities for system  
123 integration with reactions to form innovative membrane reactors [17]. Recently,  
124 significant progress has also been achieved in preparing ultrathin zeolite/MOF  
125 membranes from their 2D nanosheets and further improving their membrane flux  
126 [18,19]. For example, ultrathin (<50 nm) zeolite (SAPO-34) nanosheets seeding  
127 layer allows the production of defect-free zeolite nanofilms (500–800 nm), which  
128 displayed an exceptional orientation and facilitated transport [20]. The  
129 performance was calculated as CO<sub>2</sub> permeance of  $\approx 1.0 \times 10^{-5}$  mol (m<sup>2</sup> s Pa)<sup>-1</sup>,  
130 together with high CO<sub>2</sub>/CH<sub>4</sub> and CO<sub>2</sub>/N<sub>2</sub> selectivity of 135 and 41, respectively, in  
131 equimolar binary mixtures at room temperature. Thin membranes based on  
132 lamellar SAPO-34 zeolite nanosheets were also effective in separating  
133 CO<sub>2</sub>/CH<sub>4</sub> (selectivity=102) with a permeance of  $2.5 \times 10^{-6}$  mol (m<sup>2</sup> s Pa)<sup>-1</sup>  
134 (approximately 7500 GPU) [21].

135  
136 **Fig. 2** shows H<sub>2</sub>/CO<sub>2</sub> and CO<sub>2</sub>/N<sub>2</sub> separation performance from the state-of-the-  
137 art zeolite/MOF membranes and their comparisons with the upper bound of  
138 polymeric membranes. As can be seen, zeolite/MOF membranes have had great  
139 success for the separation of H<sub>2</sub>/CO<sub>2</sub> but much less for CO<sub>2</sub>/N<sub>2</sub> when compared

140 with polymer membranes. The reason is that in the H<sub>2</sub>/CO<sub>2</sub> system the two  
141 transport properties that determine the membrane performance – diffusion and  
142 adsorption – often have opposite effects. That is, diffusion favours hydrogen  
143 because of its smaller kinetic size, but adsorption prefers CO<sub>2</sub> because of its  
144 higher quadrupole moment. Hence, to achieve a good H<sub>2</sub>/CO<sub>2</sub> selectivity, the  
145 diffusion selectivity must be high. As said, zeolite/MOF membranes have a  
146 significant advantage over polymeric membranes in molecular sieving.

147 In contrast, in the system of CO<sub>2</sub>/N<sub>2</sub>, both diffusion and adsorption facilitate the  
148 transport of CO<sub>2</sub>. Polymers can be easily grafted with a high density of functional  
149 groups to enhance CO<sub>2</sub> adsorption and thus can achieve comparable  
150 performance to zeolite/MOF membranes. In certain conditions when the CO<sub>2</sub>  
151 affinity is strong and the temperature is low, CO<sub>2</sub> may condense inside the pores  
152 due to the capillary condensation effect. This blocks the transport of other gases  
153 and turns the membrane to be CO<sub>2</sub> selective. Most of the membranes that work  
154 well for CO<sub>2</sub>/N<sub>2</sub> are also suitable for CO<sub>2</sub>/CH<sub>4</sub>, and the selectivity is typically higher  
155 because CH<sub>4</sub> has a larger molecular size than N<sub>2</sub> [22], e.g., face-centred cubic  
156 (fcc)-MOF/polymer hybrid membranes have exhibited exceptional separation  
157 performance for energy-intensive separations considering distinct gas pairs,  
158 including H<sub>2</sub>/CH<sub>4</sub>, CO<sub>2</sub>/N<sub>2</sub>, CO<sub>2</sub>/CH<sub>4</sub> and N<sub>2</sub>/CH<sub>4</sub> [23].

159

160 Despite not yet reaching the same success as for H<sub>2</sub>/CO<sub>2</sub> separation, MOF  
161 membranes still hold a great potential to separate CO<sub>2</sub>/N<sub>2</sub>. One way is to tune the  
162 pore size to enhance the molecular sieving. In this sense, the exploration of new  
163 MOF building blocks and different topological connections should be beneficial.  
164 Another way is to improve the density of functional groups inside the MOF

165 channels to increase CO<sub>2</sub> adsorption. When looking at the history of zeolite  
166 development, most stable zeolites were discovered in the early stage. This is not  
167 surprising because zeolite synthesis is a dynamic process that tends to form the  
168 most thermodynamically stable state. This trend may also apply to MOF  
169 development and the MOF research community has grown to a substantial mass,  
170 but most of the reported MOF systems can hardly pass the stability criteria for  
171 practical applications [24]. Hence, starting from the stable MOF systems and  
172 conducting surface modification should be more efficient.

173

## 174 *2.2. Challenges in commercialization*

175 Membrane selectivity and permeance, membrane fabrication cost, long-term  
176 stability and process reproducibility determine the commercialization potential of  
177 a membrane system. The required selectivity is a process parameter that is  
178 determined by the separation task. It is also the main parameter that determines  
179 the process energy consumption. The higher the selectivity, the **lower the** energy  
180 consumption. Membrane permeance and fabrication cost determine the capital  
181 cost. **Higher** membrane permeance implies less membrane area, and thus can  
182 tolerate higher fabrication cost. **For CO<sub>2</sub>/N<sub>2</sub> separation, a selectivity of 30 and a**  
183 **permeance of 1000 GPU are the estimated polymeric membrane performances**  
184 **to make the process economically viable [25].** The fabrication cost of MOF/zeolite  
185 membranes **is** so far orders of magnitude higher than that of polymeric  
186 membranes. Hence, an equivalent improvement in permeance is required to  
187 make the process competitive. The membrane lifetime is another critical factor to  
188 determine the membrane cost. A typical lifetime is two years. The process  
189 reproducibility is a key parameter for product yield and quality control.





190

191 Factors, such as the need for robust support, lengthy and multi-step synthesis  
192 processes in batch mode, harsh synthesis conditions, such as high temperature  
193 and high pressure, and special care needed to handle the brittleness, make the  
194 fabrication cost of zeolite and MOF-based membranes much higher than that of  
195 polymeric membranes. These challenges encourage the implementation of low-  
196 cost polymeric supports and the development of fast, mild, and continuous  
197 fabrication processes, while the related cost disadvantage must be compensated  
198 by better membrane performance. For zeolite membranes, this can be  
199 compensated further by better long-term stability. For instance, high-silica  
200 zeolites are much more stable than their low-silica counterparts. Besides the Si/Al  
201 ratio, the amount of crystal surface defects and Brønsted acid sites are also key  
202 factors. A common approach to improve the hydrothermal stability is through  
203 surface modification using  $\text{SiCl}_4$  or silane to eliminate the surface defects [26].  
204 Compared to zeolites, MOFs are much weaker and more sensitive to moisture.  
205 Chemical modification to make the surface more hydrophobic is a helpful  
206 approach to improve stability [27]. However, most of the stability studies are  
207 examined only in weeks' time, which is too short to be practically meaningful.  
208 More comprehensive characterizations of the structure change (e.g., X-ray  
209 diffraction and microporosity) under relevant practical conditions in a much longer  
210 period (> 2 months) are highly demanded.

211

212 The process reproducibility of most zeolite and MOF membranes is still far below  
213 the satisfactory level. One of the major reasons is the presence of defects within  
214 the fabricated membranes. For zeolite membranes, most of the defects are



215 introduced during the thermal treatment stage, when the organic structure-  
216 directing agents are removed [28]. MOF membranes have a similar issue when  
217 the organic solvent is removed from the structure. Some innovative methods  
218 using reactive agents, such as ozone, UV, and plasma, have shown good  
219 potential to activate the membrane without crack formation [29]. However, how  
220 to implement these approaches on large scale and at a low cost is still a big  
221 challenge. Reducing the membrane thickness can help expose the structure-  
222 directing agents to the reactive agents and remove them with less difficulty.  
223 Hence, the recent development in 2D membranes (see details in section 3)[30,31]  
224 will help to improve not only the membrane permeance but also the process  
225 reproducibility. Alternatively, surface coating using rubbery polymers, such as  
226 PDMS, has been widely used in polymeric membranes as an effective defect  
227 remedy method. it has also proved to be very helpful in MOF membranes [32].  
228 Reducing the membrane permeance, this method is a necessary step in a  
229 commercial fabrication process to improve the membrane reproducibility because  
230 of its low cost and simplicity.

231

232 The commercialization of zeolite/MOF membranes will be also affected by the  
233 supports' geometry as it will subsequently determine the type of membrane  
234 modules. Most of the reported zeolite/MOF membranes in the academic literature  
235 are prepared on flat sheet supports because of their easy availability. However,  
236 all the commercial zeolite membranes so far are prepared on tubular supports.  
237 Tubular supports are more robust under pressure, easy to scale up and clean,  
238 but they are also very expensive (> 300 USD/m<sup>2</sup>) and have a low packing density  
239 (30~50 m<sup>2</sup>/m<sup>3</sup>). Compared to tubular supports, hollow fibers (HFs) share a similar



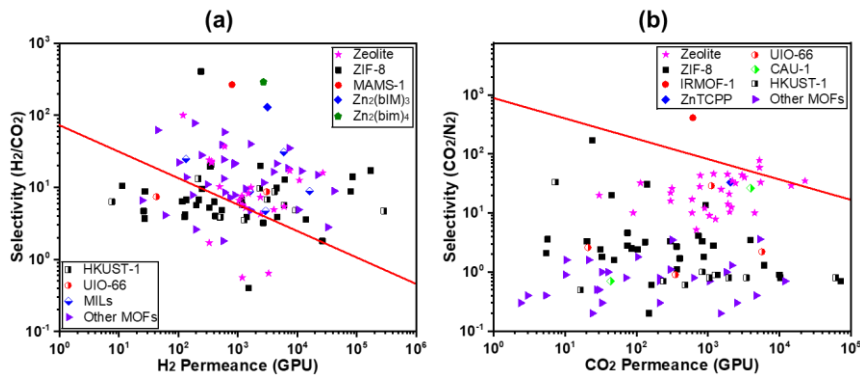
240 geometry but have a much higher packing density (see section 5), thus potentially  
241 reducing the overall cost substantially. Hence, future studies should focus more  
242 on how to integrate the membrane fabrication process more effectively with HF  
243 supports.

244 So far, there is no zeolite/MOF membrane commercialized for gas separations,  
245 but a number of zeolite membranes are on the commercialization roadmap,  
246 including those with the LTA, MFI, FAU, CHA, and DDR structures [33]. The most  
247 promising MOF membranes for commercialization are ZIF-8 and UiO-66  
248 membranes, primarily because they are so far the most stable MOF structures  
249 [34]. Moreover, ZIF-8 is made from low-cost precursors and so has a cost  
250 advantage over many other MOFs. Many economical and simple membrane  
251 fabrication approaches have been developed, such as counter diffusion [35] and  
252 electrical field-induced growth [36–38] under the aqueous solutions. However,  
253 the process reproducibility is still low and the mechanical stability under the  
254 industrially relevant pressures (> 15 bar) has not been demonstrated.

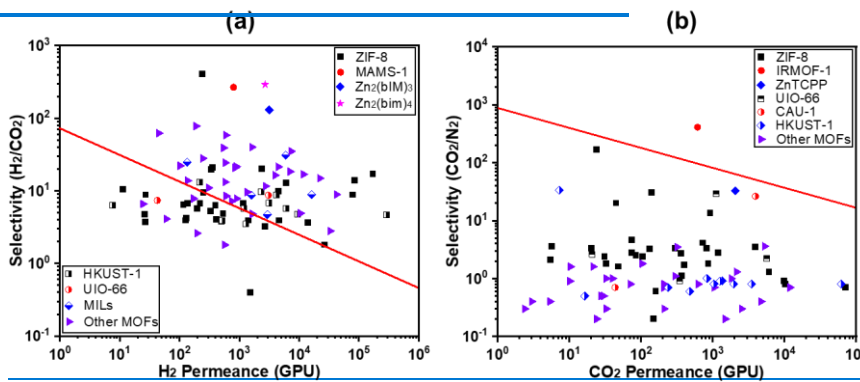
255

256 Some zeolite membranes, such as LTA zeolite [39], have been successfully  
257 commercialized in liquid separation, which has certainly enhanced the confidence  
258 in overcoming the abovementioned challenges in gas separation. With more  
259 industrial experiences accumulated in zeolite membranes, it is expected that the  
260 production cost will be significantly reduced, and the membrane quality and  
261 process reproducibility will be greatly improved. As the syntheses of zeolite/MOF  
262 membranes share many common features, these signs of progress will certainly  
263 speed up the commercialization activities of the entire field in the near future.





264



265

266 **Fig 2.** Separation performances of zeolite/MOF membranes and their  
 267 comparisons with the upper bound of polymer membranes. (a) For H<sub>2</sub>/CO<sub>2</sub> and  
 268 (b) for CO<sub>2</sub>/N<sub>2</sub>. The red lines in the diagram represent the upper bound of  
 269 polymeric membranes, where a membrane thickness of 100 nm is used to  
 270 convert the permeance from the permeability database of polymeric gas  
 271 separation membranes [40]. The data points of zeolite/MOF membranes are  
 272 adapted from Ref.[41]

273

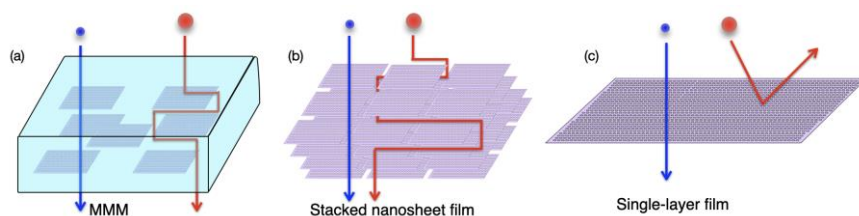
### 274 3. 2D nanoporous materials for gas separation membranes

#### 275 3.1. Opportunities of 2D materials for gas separation

Con formato: Español (España)

276 Nanoporous materials with a 2D morphology have the unique potential to  
277 constitute the thinnest selective layers ever imagined, down to the thickness of  
278 an atom, and therefore, can maximize the permselective gas flux reducing the  
279 needed membrane area and associated capital cost. Three distinct designs for  
280 selective layers can be achieved (**Fig. 3**): MMM where 2D materials constitute an  
281 ideal filler in a polymer matrix; stacked nanosheet membranes; and single-layer  
282 2D film.

283



285 **Fig 3.** Design approaches for the selective layer from 2D materials and  
286 corresponding molecular pathways. a) MMM prepared by dispersing 2D  
287 nanosheets inside a polymeric filler. b) Stacked nanosheet film by the assembly  
288 of nanosheets. c) Macroscopic single-layer 2D film.

289

290 MMM prepared using nanoporous 2D nanosheets are extremely attractive due to  
291 the high aspect ratio and nanoscale thickness of the nanosheets. This is because  
292 a preferential orientation of the nanosheets in the matrix can be obtained, filler  
293 loading in the matrix can be maximized, and the overall film thickness can be  
294 minimized. The emergence of nanoporous 2D materials with high interphase  
295 compatibility with polymer (MOFs [42], g-C<sub>3</sub>N<sub>4</sub> [43], covalent organic frameworks  
296 [44], etc.) have led to MMM yielding improved separation performances  
297 compared to the upper bound for polymeric materials. While membranes based

298 on stacked 2D nanosheet films as the selective layer offer performance  
299 advantages over nanosheet-based MMM. The stacked nanosheet film offers a  
300 nanoporous pathway across the entire selective layer, improving the diffusivity of  
301 the gas molecules.

302

303 Oriented nanosheet films can be achieved by a scalable technique such as  
304 filtration on a porous support, and the film thickness can be easily regulated by  
305 the amount of suspension. The separation performance from the stacked  
306 nanosheet film is determined by the interplay between two transport pathways;  
307 one constituted by the nanosheet porosity and the other by the intersheet or  
308 packing gap between the nanosheets. This gap needs to be small enough to not  
309 become the primary transport pathway but also large enough so that the pore  
310 openings of the nanosheets are not blocked in the turbostatically-stacked film.  
311 Approaches modulating the gap, e.g., hot drop coating and reactive condensation  
312 of the nanosheets have yielded promising H<sub>2</sub>/CO<sub>2</sub> separation performance from  
313 MOF nanosheets [18] and more recently from zeolite nanosheets [19].  
314 Impervious nanosheets, such as graphene oxide [45] and MXenes [46], have also  
315 shown promising performance from their stacked films where gas transport takes  
316 place through the intersheet gap. For example, graphene oxide nanosheets  
317 assembled into laminar structures have displayed fast and CO<sub>2</sub> selective  
318 transport channels (CO<sub>2</sub>/N<sub>2</sub>: 91), along with exceptional operational stability [47].  
319 Unfortunately, the intersheet gap and the gas transport in these films are sensitive  
320 to operating conditions including feed pressure and humidity [48,49], affecting the  
321 separation performance.



322 Synthesis of 2D nanosheets hosting CO<sub>2</sub>-sieving nanopores will allow the  
323 realization of high-performance MMMs for CO<sub>2</sub> separation. A potential pathway  
324 is **the** exfoliation of a suitable layered precursor, such as zeolite hosting **an** 8-  
325 membered silicate ring. Layered SAPO-34 has been recently reported [21].  
326 Recently, synthesis of 20-nm-thick SAPO-34 nanosheets have been also  
327 reported [20]. Layered SAPO-34 has been recently reported [21], including its  
328 exfoliation to single-layer sheets [20]. Another promising material for this is  
329 ordered *g*-C<sub>3</sub>N<sub>4</sub> such as poly(triazine imide) (PTI) which hosts 3.4 Å pores.  
330 Recently, PTI nanosheets have been prepared **as** single-layer nanosheets [43],  
331 however, the lateral size of exfoliated nanosheets was small (<50 nm), and the  
332 yield of exfoliated nanosheets was low. Synthesis of high-aspect-ratio *g*-C<sub>3</sub>N<sub>4</sub>  
333 nanosheets with high yield would be highly beneficial in this respect.

334

335 Macroscopically-large 2D films, such as graphene and analogues, can be used  
336 to fabricate membranes with a selective layer that is just one atom thick. When a  
337 high density of gas-sieving pores **is** incorporated in graphene, extremely large  
338 permselective gas flux can be realized [50]. Molecular simulations predict  
339 permselective CO<sub>2</sub> permeance in the range of 10000-100000 GPU [51]. A CO<sub>2</sub>  
340 permeance of 10000 GPU has been recently demonstrated in combination with  
341 an attractive CO<sub>2</sub>/N<sub>2</sub> selectivity (>20)[51,52]. This is mainly because of the  
342 extremely short diffusion **path length** of gases across the atom-thick pores of  
343 graphene [53]. Gas sieving can be obtained from nanopores hosting electron  
344 density gap comparable to that of the target gas molecules. For such nanopores,  
345 the flux of gas molecules can be modelled using the transition state theory and is  
346 determined by the energy barrier experienced by the molecule while crossing the

Con formato: Fuente: Sin Cursiva, Color de fuente:

Con formato: Color de fuente: Rojo

347 nanopore [54]. As a result, the relative size of the gas molecules with respect to  
348 the nanopore determines the gas pair selectivity.

349

350 There are three key challenges in developing size-sieving nanoporous graphene  
351 membranes: angstrom-scale pores have to be created with dimensions able to  
352 sieve the desired components (e.g., CO<sub>2</sub> or H<sub>2</sub>); pore creation technique has to  
353 be precise to yield a narrow pore size distribution avoiding large nonselective  
354 pores; and the density of gas-permeable pores should be high enough (>0.1%)  
355 to outperform the conventional membranes. Meeting these requirements would  
356 realize membranes, which are highly permeable but also selective, overcoming  
357 the selectivity-permeability trade-off of conventional polymeric membranes. This  
358 will require the development of synthetic approaches where pore nucleation and  
359 expansion can be controlled, e.g., down to the removal of 10-16 carbon atoms  
360 per pore in the case of graphene for H<sub>2</sub>- and CO<sub>2</sub>-sieving [52].

361

362 The control of pore density (nucleation) and size (expansion), permitting  
363 maximization of gas flux and gas pair selectivity, will be highly beneficial. For  
364 CO<sub>2</sub>/N<sub>2</sub> separation, exploiting the higher adsorption affinity of CO<sub>2</sub> by  
365 functionalizing with CO<sub>2</sub>-philic groups is an attractive approach [55,56]. Although  
366 the field is in its infancy, attractive separation performance has been  
367 demonstrated for applications where large permeance is desired along with a  
368 moderate selectivity, e.g., post-combustion carbon capture. For instance,  
369 nanoporous graphene membranes prepared by controlled pore formation and/or  
370 functionalization have yielded CO<sub>2</sub> permeances of 10000 GPU along with an  
371 attractive CO<sub>2</sub>/N<sub>2</sub> selectivity (above 20)[57]. Advances on the fundamental fronts





372 – especially mechanistic understanding of nanopore formation – are expected to  
373 further improve the separation performance toward improving the gas pair  
374 selectivity.

375

### 376 *3.2. Challenges in commercialization*

377 A challenge for MMM and stacked nanosheet films is to develop strategies to  
378 reduce their thickness down to that of the selective layer in TFC (<100 nm). For  
379 this, the development of low-cost, smooth, and porous polymeric support hosting  
380 asymmetric porous structure with nanometer-scale pore opening will be highly  
381 attractive. Such a support structure would allow the formation of a uniform thin  
382 film while avoiding pinhole defects. Nonsolvent-induced phase separation of  
383 polymer is a promising technique to produce such porous supports. In cases  
384 where high thermal stability is required, high-glass-temperature polymers, such  
385 as polybenzimidazole [58], are attractive.

386

387 In the case of single-layer 2D films such as nanoporous graphene film, a key  
388 challenge lies in developing synthetic methods that are conducive to scale-up.  
389 Large-area polycrystalline graphene films can be synthesized on a metal foil by  
390 chemical vapor deposition (CVD), a scalable method that can produce hundreds  
391 of meter squares of graphene, e.g., by a continuous roll-to-roll process [59] or by  
392 stacking the metal foil [60]. However, the CVD technique has to be optimized to  
393 yield graphene at a large scale with high enough quality for membranes, i.e., with  
394 an extremely low density of defects and contaminations. The cost of catalytic  
395 metal foil used for CVD of graphene needs to be reduced to or lower than 10



396 \$/m<sup>2</sup>. Alternatively, methodologies allowing the reuse of the foil for several rounds  
397 of synthesis can cut down the effective cost of foil.

398

399 For nanoporous single-layer graphene membrane, another critical challenge is  
400 the scalable incorporation of nanopores into an otherwise impermeable graphitic  
401 lattice. Direct synthesis of nanoporous graphene is highly attractive in this regard  
402 (top-down approach). Proof-of-concept for this has been demonstrated by  
403 lowering the CVD temperature [61,62] or by controlling the amount of carbon  
404 precursors for the synthesis of graphene [63]. For pore incorporation by post-  
405 synthetic etching (bottom-up approach), scalable chemical etching techniques  
406 involving gaseous etchants are highly attractive. Reactive gases can be exposed  
407 uniformly over the surface of graphene in simple setups. However, controlling  
408 pore nucleation and expansion at the Å-scale in an industrial-sized reactor is  
409 expected to be challenging for both top-down and bottom-up approaches. An  
410 improved mechanistic understanding of events, which control pore-size  
411 distribution, is needed to achieve a high pore density with a narrow size  
412 distribution.

413

414 From a membrane fabrication perspective, a crucial challenge is to develop  
415 methods for transferring the graphene film onto a porous support without inducing  
416 cracks or tears in the film. CVD graphene is synthesized on a substrate, and the  
417 transfer of graphene involves its isolation from the growth substrate. The  
418 mechanical stress generated during the isolation step is often high enough to  
419 generate macroscopic cracks in graphene, which deteriorates gas pair selectivity.  
420 Recently, crack-free centimeter-scale graphene membranes have been

421 demonstrated by permanently reinforcing graphene with a gas-permeable layer,  
422 such as nanoporous carbon film [64], carbon nanotube film [65] and dense  
423 polymer films [52]. However, these methods require further improvement for the  
424 preparation of graphene membranes on low-cost and flexible support, such as  
425 those used for the preparation of polymeric TFC membranes.

426

#### 427 **4. Current technical limitations of asymmetric membranes presenting a** 428 **selective layer with nanoporous materials**

##### 429 *4.1. Asymmetric membranes for gas separation*

430 In general, dense and thick polymeric membranes with no porous structure are  
431 mostly applied for characterization purposes or to test new membrane materials.  
432 Their single-gas permeability and ideal selectivity for a given mixture can be  
433 obtained with the so-called time lag system with the advantage of allowing the  
434 estimation of diffusivity and solubility parameters of the membrane [66]. However,  
435 this experimental setup is not very realistic, as in real-world applications mixtures  
436 of gases are used, including minor components such as moisture or H<sub>2</sub>S,  
437 depending on the origin of the stream to be treated.

438

439 Instead, asymmetric membranes with a selective skin layer on top of a  
440 mechanically stable support constitute the perfect membrane structure, and one  
441 which could be ideal for commercial applications. The advantage of asymmetric  
442 membranes is that transport resistance is minimised and fabrication costs are  
443 reduced by using the minimum amount of selective material. This type of  
444 membrane supposes two in-series resistances to the gas transport and the  
445 contribution of the support has to be minimum so as not to penalize the function



446 of the selective film [67]. As a consequence, the porosity of the support has to be  
447 as high as possible while providing an adequate activated surface to favour the  
448 deposition of the ultrathin film by certain coating techniques [2].

449

450 Sometimes an intermediate gutter layer is placed between the previous two  
451 layers. A gutter layer is an intermediate layer between the top selective layer and  
452 the surface of the membrane support. The gutter layer can modify the surface  
453 defects, plug the pores of membrane substrate and prevent the selective coating  
454 dispersion from penetrating deeply into the pores. It also provides a smooth  
455 surface bed for the top selective layer so that it is easier to spread a thinner layer  
456 than to coat directly on the relatively rough substrate. As a result, the gutter layer,  
457 even if it contributes to the whole transport resistance, can enhance the overall  
458 permeance of the membrane by an order of magnitude [68], having found that  
459 the gutter layer permeability should be 5-10 times higher than that of the selective  
460 layer to minimize the decrease in selectivity [69].

461

#### 462 *4.2. Limitation of support*

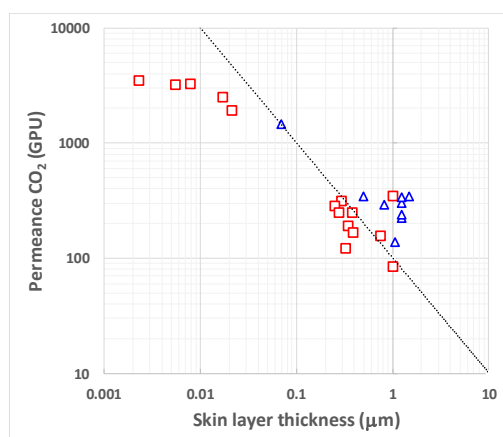
463 In addition to conferring mechanical stability to the membrane, the support, in  
464 series with the skin layer, should minimally restrict the membrane transport. As  
465 an example, PEBA (poly (ether-block-amide)) type polymers, commercialized as  
466 Pebax<sup>®</sup>, are some of the most studied skin layers for CO<sub>2</sub> selective membranes.

467

468 **Fig. 4** illustrates the expected effect of the membrane thickness on the  
469 permeance for elastomeric Pebax<sup>®</sup> 1657 membranes. From nine relevant  
470 studies, an average CO<sub>2</sub> permeability of 101±34 Barrer was obtained for Pebax<sup>®</sup>



471 1657 thick dense membranes (corresponding to CO<sub>2</sub>/N<sub>2</sub> selectivities in the 36-89  
472 range) [67,70–77]. The dotted line of negative slope is the calculation of  
473 permeance as a function of skin layer thickness from the value of 101 Barrer  
474 (dividing permeability by membrane thickness), implying negligible resistances  
475 from the support and gutter layer. Even if gas separation supports are highly  
476 permeable (ca. 200,000 GPU of CO<sub>2</sub>) [78,79], in practice, the TFC membranes  
477 of only Pebax® 1657 (red squares) exhibit lower permeances than expected due  
478 to the negative contributions of both the support and the gutter layer. The  
479 deviation augments with decreasing selective layer thickness. The blue triangles  
480 in the plot correspond to Pebax® 1657 based MMMs, always with permeances  
481 above the expected, in line with the capacity of fillers to enhance the permeation  
482 of such membranes [80]. From this plot, we can conclude that as the skin layer  
483 thickness goes down to the nanometer dimension, the resistance of the support  
484 becomes more relevant suggesting its improvement in terms of porosity,  
485 thickness and mechanical strength. Moreover, MMMs can enhance the  
486 permeance beyond the thickness-related value.



487



488 **Fig. 4.** CO<sub>2</sub> permeance as a function of the thickness of the Pebax® 1657  
489 selective layer for different TFC membranes. The dotted line was obtained from  
490 the average of the permeabilities of nine different dense membranes [67,70–77].  
491 The red squares and blue triangles correspond, respectively, to bare polymer  
492 [67,81–85] and to filler modified [69,85–87] TFC membranes of different  
493 thicknesses. These membranes are known as TFN membranes, i.e. TFC  
494 membranes incorporating porous particles. When the membrane thickness is 1  
495 μm, a permeance of 1 GPU (1 GPU= 1·10<sup>-6</sup> cm<sup>3</sup>(STP)·cm<sup>-2</sup>·cmHg<sup>-1</sup>·s<sup>-1</sup>)  
496 corresponds to a permeability of 1 Barrer.

497

#### 498 *4.3. Further developments in gutter layer and support*

499 The highest permeance gas separation membrane ever reported, with 40,000  
500 GPU of CO<sub>2</sub> and 10-12 CO<sub>2</sub>/N<sub>2</sub> selectivity, was made of PDMS [79]. This  
501 membrane was 34 nm thick and prepared onto a glass substrate by spin coating,  
502 which was later detached using ethanol and thus transferred onto highly  
503 permeable PAN (polyacrylonitrile) ultrafiltration support; in this way, it was  
504 avoided the use of a gutter layer and the possible penetration of the PDMS within  
505 the substrate pores. Indeed, to extract the maximum performance of the selective  
506 layer, the resistances of the gutter layer and support have to be as negligible as  
507 possible.

508

509 The typical approach is to fill the support porosity with some liquid to avoid the  
510 penetration of the gutter material [78,88], but there are other interesting  
511 approaches such as the use of sacrificial gutter layers [67,89]. In this case, the  
512 sacrificial material should be removed without altering either the membrane

513 separation properties or its attachment to the support. The PDMS membrane  
514 mentioned previously with the 40,000 GPU CO<sub>2</sub> permeance was first prepared  
515 by spin coating on a sacrifice layer of poly(4-hydroxystyrene)[79]. This was  
516 dissolved in ethanol and then the PDMS transferred to a PAN support maintaining  
517 its shape and mechanical strength. Even if it is true that the extrapolation of this  
518 methodology to a scalable industrial procedure and with more selective polymers  
519 than PDMS (this is more a gutter layer material than a desirable selective  
520 polymer, at least for CO<sub>2</sub> separation) may not be immediate, these results are  
521 quite encouraging. In fact, with this principle, a 70 nm thick polyetheramine-  
522 graphene oxide Pebax 1657 membrane has been prepared on a 75 nm thick  
523 PDMS gutter layer showing a CO<sub>2</sub> permeance of 1455 GPU together with a  
524 CO<sub>2</sub>/N<sub>2</sub> selectivity of 68.1 [69]. In addition, one of the most promising membranes  
525 for CO<sub>2</sub> separation is the Polaris™ one, made of a proprietary polymer presenting  
526 a gutter layer strategy and commercialized by Membrane Technology and  
527 Research, Inc., with up to 2000 GPU of CO<sub>2</sub> and CO<sub>2</sub>/N<sub>2</sub> selectivity of 50 [90,91].

528

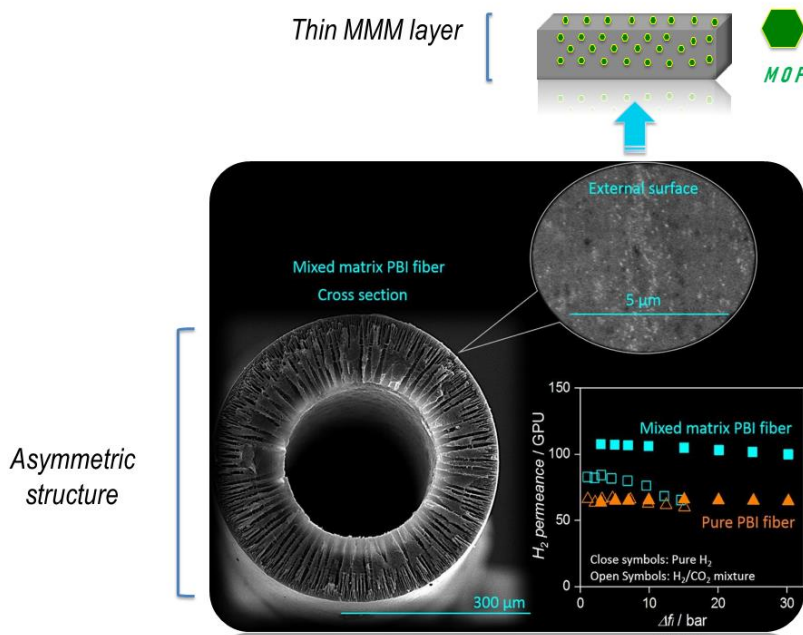
## 529 **5. Membrane configurations and process requirements**

530 To further improve the separation properties of thin layers, several microporous  
531 materials (like MOF) with exceptional molecular sieving ability are being filled in  
532 a composite (or MMM) layer onto HFs (see **Fig. 5**). However, **a non-compelling**  
533 **physical and chemical compatibility among inorganic and organic phases in**  
534 **composites may compromise the result of enhanced separation performance.** In  
535 the future, particular emphasis should be placed on the resulting structural  
536 changes to the membrane formulation when extrapolated from flat to HF  
537 configuration.



538

539



540

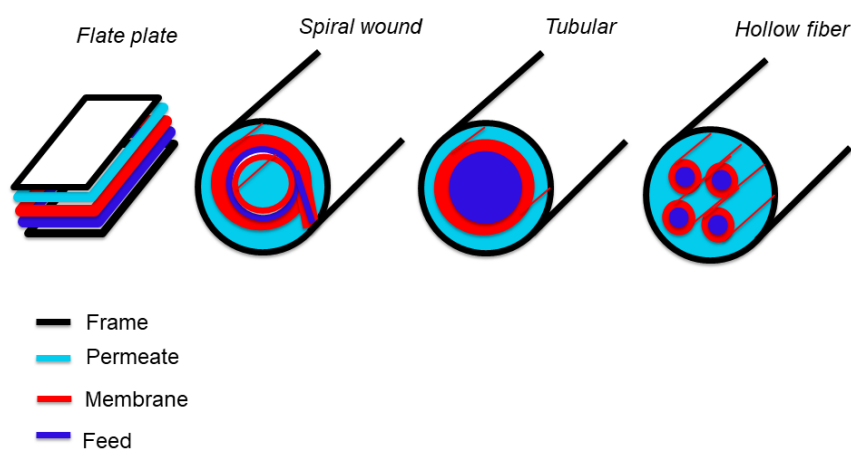
541 **Fig. 5.** Composite hollow fibre membranes for gas separation. Cross-section view  
542 of polybenzimidazole-10 wt.% ZIF-8 mixed matrix asymmetric hollow fibre for  
543 H<sub>2</sub>/CO<sub>2</sub> separation [92].

544

545 Asymmetric membranes can be manufactured in a flat or a HF geometry and then  
546 packed into modules to reach high **productivity** for industrial applications. **Fig. 6**  
547 graphically illustrates the types of membrane module configurations, which  
548 typically refer to the geometry of the membrane and its position in space in  
549 relation to the flow of the feed fluid and of the permeate. HF [93] and spiral wound  
550 [87] are the membrane configurations providing the highest values of  
551 intensification in terms of membrane area per module volume (i.e., packing



552 density). HF modules stand out as the most preferred due to their high packing  
553 density, varying from 500 up to 9000 m<sup>2</sup> m<sup>-3</sup>, exceeding the reported densities for  
554 spiral-wound modules (ca. 1200 m<sup>2</sup> m<sup>-3</sup>) and plate and frame modules (ca. 100–  
555 400 m<sup>2</sup> m<sup>-3</sup>) [94]. HF membranes also have the benefit of being able to handle  
556 extremely high transmembrane pressure difference (approximately 70 bar), while  
557 the fabrication cost is around 5–20 times lower than the equivalent for spiral  
558 wound modules [95].



559

560 **Fig. 6.** Graphical depiction of the four types of membrane configurations.

561

562 Most commercially available membranes are manufactured as HF modules, while  
563 less than 20% correspond to spiral wound modules. Both are most suitable for  
564 gas separation applications [96], as they are relatively less prone to membrane  
565 fouling than flat sheet or tubular modules. In general, HF modules experience  
566 25% more membrane surface shears promoting hydrodynamic pattern changes  
567 which consequently mitigate the deposition of foulants, e.g., when operating HF  
568 modules in cross-flow filtration mode, shear forces on the membrane occur  
569 thanks to bubbling, vibration, or particle scouring [97]. However, in the case of

570 HF modules, the feed gas requires further pre-treatment to mitigate severe fouling  
571 and plasticization, depending on the type of material. As for spiral wound  
572 modules, apart from being more resistant to plasticization, can be applied to a  
573 wider range of membrane materials compared with HFs [95]. To date, few spiral  
574 wound membranes for gas separation (at least for CO<sub>2</sub> and H<sub>2</sub>-containing  
575 mixtures) have been documented [98–100].

576

577 Today, the production of HFs with a selective layer is still challenging for gas  
578 separation since gas molecules are sized in the Angstroms range [101], and are  
579 therefore very sensitive to any defect in the functional layer. The usage of an  
580 atomically thin layer with precisely controlled pores and chemical functionality is  
581 crucially needed to achieve true molecular sieving of gas molecules [102], as this  
582 separation mechanism is usually compromised by surface adsorption and  
583 condensation phenomena of the gas molecules in the membrane pores [103].

584

585 Forming ultrathin membranes into HF modules is an ongoing research challenge,  
586 but they still represent a promising way for efficient gas separation with scalable  
587 productivity and less economic expenditure [96]. Various ultrathin composite HF  
588 membranes for CO<sub>2</sub>/H<sub>2</sub> separation have been successfully synthesized at lab  
589 scale (Table 1). MOFs (such as ZIF-8, Cu<sub>3</sub>(BTC)<sub>2</sub>, MIL-53 and UiO-66-NH<sub>2</sub>) are the  
590 most reported nanoporous fillers in composite HF fabrication due to their physical  
591 and chemical compatibility with polymer phases; however, such membrane  
592 modules are limited to small membrane sizes of 10-48 cm length.

593

594



**Table 1.** Various hollow fibre (HF) membrane concepts aimed at separating CO<sub>2</sub> and H<sub>2</sub> containing mixtures.

<i>Composition</i>	<i>Type of HF</i>	<i>Membrane/module size</i>	<i>Gas mixture</i>	<i>Operating conditions</i>	<i>Permeance in GPU (of faster gas)</i>	<i>Selectivity</i>	<i>Reference</i>
ZIF-8/UiItem®	Mixed matrix	6 fibers/ 20 cm length each	CO <sub>2</sub> /N <sub>2</sub>	45 °C, 6.8 bar	34	28	[104]
PTPESU	Asymmetric	10 fibers/ 15 cm length each	CO <sub>2</sub> /N <sub>2</sub>	25 °C, 3.5 bar	85.1	34	[105]
PBI/P84	Asymmetric	1 fiber/ 17 cm length	H <sub>2</sub> /CO <sub>2</sub>	180 °C, 6 bar	90	13.5	[106]
Pebax/PDMS/PAN	Composite	1 fiber/ 15-20 cm length	H <sub>2</sub> /CO <sub>2</sub>	25 °C, 2 bar	59.8	8.1	[107]
PVA/PPO	Thin composite	film 10 fibers/ 10 cm length each	CO <sub>2</sub> /N <sub>2</sub>	25 °C, 2 bar	791	40	[108]
PDMS/PAN	Thin composite	film 1 fiber/ 15 cm length	CO <sub>2</sub> /N <sub>2</sub>	25 °C, 3 bar	5000	11	[109]
sPPSU/PBI	Dual-layer	1 fiber/ 15 cm length	H <sub>2</sub> /CO <sub>2</sub>	90 °C, 14.2 bar	16.7	9.7	[110]
TNTs/PSf	Mixed matrix	10 fibers/ 20 cm length each	CO <sub>2</sub> /N <sub>2</sub>	25 °C, 3 bar	120	28.8	[111]
ZIF-8/PBI	Mixed matrix	1-22 fibers/ 18 cm length each	H <sub>2</sub> /CO <sub>2</sub>	150 °C, 7 bar	107	18	[92]



<b>ZIF-8/Si<sub>3</sub>N<sub>4</sub></b>	Ceramic	1 fiber/ 10 cm length	H <sub>2</sub> /CO <sub>2</sub>	25 °C, 2.5 bar	2505	11.7	[112]
<b>PDMS-</b>	Asymmetric	1 fiber/ 15 cm length	CO <sub>2</sub> /N <sub>2</sub>	25 °C, 5 bar	109	31	[113]
<b>Cu<sub>3</sub>(BTC)<sub>2</sub>/PSf</b>							
<b>PEI/Aminosilane functionalized MIL-53</b>	Mixed matrix	10 fibers/ 48 cm length each	CO <sub>2</sub> /N <sub>2</sub>	35 °C, 5 bar	30.9	34.7	[114]
<b>PIM/PDMS/PAN</b>	Asymmetric composite	3 fibers/ 16 cm length each	CO <sub>2</sub> /N <sub>2</sub>	25 °C, 2 bar	483	22.5	[115]
<b>Pebax® 2533-UiO-66-NH<sub>2</sub>/PP</b>	Mixed matrix	1 fiber/ 7-10 cm length	CO <sub>2</sub> /N <sub>2</sub>	25 °C, 2 bar	26	37	[116]

596 *Abbreviations:* PTPEU (poly trimethyl phenylene ethersulfone); PBI (polybenzimidazole); sPPSU (sulfonated polyphenylsulfone); PVA (poly (vinyl alcohol));  
597 PDMS (polydimethylsiloxane); PAN (polyacrylonitrile); PPO (poly(p-phenylene oxide)); TNT (titania nanotube); PSf (polysulfone); PEI (polyetherimide); PIM  
598 (polymer of intrinsic microporosity); PEI (polyetherimide), PP (polypropylene).



599 Depending on the type of polymer (or dope solution composition) and preparation  
600 protocol, polymer composite HFs can display high permeation rates in gas  
601 separation performance. This is the case of PDMS/PAN thin composite, which  
602 has shown up to 5000 GPU permeance in CO<sub>2</sub>/N<sub>2</sub> mixtures [109], while  
603 PIM/PDMS/PAN HFs displayed 483 GPU (with selectivity values of 22.5) towards  
604 similar gas mixture [115]. In this HF, a cross-linked PDMS gutter layer was  
605 introduced between the PIM selective layer and the PAN substrate, which was  
606 able to mitigate the detrimental solvent effects during the dip coating, permit PIM  
607 to adhere to it, and redistribute the gas transport across the membranes.

608

609 Compared with such HFs, PDMS–Cu<sub>3</sub>(BTC)<sub>2</sub>/PSf [113] and PEI/aminosilane  
610 functionalized MIL-53 [114] HFs offered better performance with CO<sub>2</sub>/N<sub>2</sub>  
611 selectivities of 31 and 34.7, respectively, but with a decreased CO<sub>2</sub> permeance.  
612 ZIF-8 filled polyetherimide (Ultem® 1000) matrix was subsequently utilized for the  
613 fabrication of dual-layer asymmetric HF membranes via the dry jet-wet quench  
614 method [104]. The resulting MMM HFs showed a 20% increased permeance in  
615 CO<sub>2</sub>/N<sub>2</sub> testing compared with the pristine HFs. In this regard, these few  
616 examples evidence that the involvement of inorganic materials, like MOFs, with  
617 superior gas molecular sieving nature, can enhance the CO<sub>2</sub>/N<sub>2</sub> separation  
618 performance of polymer membranes [18]. Similarly, specific MOFs can be  
619 adapted in HFs presenting polymer or inorganic membrane supports for H<sub>2</sub>/CO<sub>2</sub>  
620 mixture separation. For instance, ZIF-8 has contributed to a 65% increase in H<sub>2</sub>  
621 permeance at constant ideal selectivity in PBI HFs. Unlike pristine PBI HFs, filler  
622 incorporation into the PBI matrix contributed to a substantial increase in H<sub>2</sub>  
623 permeance from 65 GPU to 107 GPU, while the ideal H<sub>2</sub>/CO<sub>2</sub> selectivity remained



624 unchanged (ca. 18)[92]. Knowing the great advantages of ceramic materials in  
625 terms of high thermal and chemical stability in harsh environments, they have  
626 started to be applied as HF supports. As an example, ZIF-8 supported on silicon  
627 nitride ceramic HF exhibited improved permeation as high as 2,505 GPU, with  
628 H<sub>2</sub>/CO<sub>2</sub> selectivity of 7.3 [112].

629 To date, most advances in composite polymer-based membranes containing  
630 either MOFs or zeolites have relied on the fabrication of flat sheet membranes,  
631 which have exhibited impressive performance surpassing polymer upper bound  
632 performance, e.g., MMMs based on ZIF-300 filled PEBA [117]. This is a result of  
633 engineered designs of the polymer and inorganic phases. Unfortunately, there is  
634 still limited research on HF membranes but studies show that they represent the  
635 most prominent membrane configuration for separating CO<sub>2</sub> and H<sub>2</sub>-containing  
636 mixtures (see **Table 1**), at least in H<sub>2</sub>/CO<sub>2</sub> and CO<sub>2</sub>/N<sub>2</sub> mixture separations with  
637 scalable performances for possible industrial purposes [96]. Certainly, several  
638 factors should be considered when tailoring a HF membrane, such as inorganic  
639 and organic (i.e., polymer) phase properties, along with their compatibility with  
640 each other.

641 To some extent, the dope solution composition has a fundamental and decisive  
642 impact on the morphology and structure of prepared membranes and thus on gas  
643 separation performance. Therefore, particular emphasis must be placed on the  
644 fabrication parameters[118]; for instance, the dry-jet wet spinning process stands  
645 out as the most used method for HF preparation, where several variables, such  
646 as bore fluid composition, flow rates of dope and bore fluids, and air gap, are  
647 essential to obtain defect-free membranes. However, as for the selection of  
648 membrane material (both the support and the selective layer), the presence of

649 humidity and impurities (e.g., H<sub>2</sub>S)[88], as well as operating temperature and  
650 pressure, are also important for targeted separations.

651

652 Since most industrial separations demand large membrane areas (ca. 1000 –  
653 millions m<sup>2</sup>), the major challenge impeding the industrialization of new membrane  
654 materials in HF configurations lies in producing membranes in a large quantity  
655 with high permeance and selectivity at a reasonable cost [119]. **Table 1** reports  
656 successful examples of new composite membranes in small HF modules;  
657 however, there is no report in which any of those membranes have been  
658 extrapolated to a **large scale**. Developing scalable methods to obtain reproducible  
659 permeance and selectivity in large HFs thus still remains highly challenging.

660

## 661 **6. Conclusions and outlook**

662 Current and future energy production processes involve **the** separation of CO<sub>2</sub>  
663 and H<sub>2</sub>-containing mixtures. In this context, membrane technology seems to be  
664 the most suitable approach from the point of view of process simplicity, cost and  
665 sustainability. Besides, membranes based on or modified with nanoporous  
666 materials have demonstrated very good performance when separating CO<sub>2</sub>/N<sub>2</sub>,  
667 CO<sub>2</sub>/CH<sub>4</sub> and H<sub>2</sub>/CO<sub>2</sub> energy-related mixtures. Nevertheless, **some limitations**  
668 **still remain to achieving the industrialization of membranes in this field, even if**  
669 **selectivity-permeance upper bounds have been surpassed with the help of many**  
670 **nanoporous materials.**

671

672 For 2D materials, such as nanoporous graphene, control of pore size and porosity  
673 can still be enhanced by **an** improved mechanistic understanding of pore



674 incorporation. The thickness decrease in the selective membrane skin layer  
675 would overcome issues like membrane activation and even the cost of relatively  
676 expensive nanoporous materials. However, large-scale, effective methods for  
677 transferring 2D films to porous supports without incurring defect formation are  
678 needed.

679 The ability to implement flat membrane procedures to process intensified spiral  
680 wound and HF membrane systems has to be improved. Moreover, some issues  
681 like support adequacy in terms of mechanical and diffusion resistances (requiring  
682 or not of a gutter layer), fabrication reproducibility and cost, mechanical  
683 robustness and long-term stability need attention to achieve commercially reliable  
684 membrane systems.

685 All these limitations suggest the concentration of efforts in two directions: more  
686 interdisciplinary work is needed combining chemistry, materials science and  
687 chemical engineering to extract the best of nanoporous materials when allied with  
688 the other membrane components; and more academic-industry collaboration is  
689 desired focussing on specific energy-relevant gas mixtures to be separated under  
690 realistic conditions.

691

#### 692 ***Recommendations for the researchers in the field***

693 For a possible real application, the gas mixtures must present contaminants (e.g.,  
694 H<sub>2</sub>S, CO), water and other gases, which strongly affect the membrane  
695 performance [120]; e.g., CO<sub>2</sub> and N<sub>2</sub> permeability can decrease as water  
696 occupies free volume in polymer membranes, while the N<sub>2</sub> permeability could  
697 increase in the presence of H<sub>2</sub>S by improving the N<sub>2</sub> solubility or diffusion within  
698 specific polymers (e.g., PDMS) [120].





699 To date, most of the research has been done at a lab-scale, therefore, there is a  
700 need of extrapolating the performance to a larger scale (e.g., pilot scale), this is  
701 related to finding scalable fabrication methods with reproducibility in membrane  
702 performance. This may also imply the handling of operating conditions for better  
703 performance. For example, as for CO<sub>2</sub> separations, feed CO<sub>2</sub> concentration  
704 influence the separation performance (particularly gas flux) since there is different  
705 CO<sub>2</sub> partial pressure across the membrane.

706 In addition to this, when testing under zero transmembrane pressure using sweep  
707 gas, the non-selective viscous flow is minimized through the membrane defects  
708 resulting in enhanced selectivity. In realistic practical conditions, a non-zero  
709 downstream pressure exists, leading to higher solute concentrations in the  
710 membrane. This aspect should be also considered when testing the membrane  
711 performance.

712

713

714

## 715 References

- 716 [1] D.S. Sholl, R.P. Lively, Seven chemical separations, *Nature*. 532 (2016) 435–  
717 437.
- 718 [2] R. Castro-Muñoz, K. V. Agrawal, J. Coronas, Ultrathin permselective  
719 membranes: the latent way for efficient gas separation, *RSC Adv.* 10 (2020)  
720 12653–12670. <https://doi.org/10.1039/D0RA02254C>.
- 721 [3] S. Kim, Y.M. Lee, High performance polymer membranes for CO<sub>2</sub> separation,  
722 *Curr. Opin. Chem. Eng.* 2 (2013) 238–244.  
723 <https://doi.org/10.1016/j.coche.2013.03.006>.
- 724 [4] R. Castro-Muñoz, M.Z. Ahmad, V. Fila, Tuning of Nano-Based Materials for

- 725 Embedding Into Low-Permeability Polyimides for a Featured Gas Separation,  
726 *Front. Chem.* 7 (2020) 1–14. <https://doi.org/10.3389/fchem.2019.00897>.
- 727 [5] D.Q. Vu, W.J. Koros, S.J. Miller, Mixed matrix membranes using carbon  
728 molecular sieves, *J. Memb. Sci.* 211 (2003) 311–334.  
729 [https://doi.org/10.1016/S0376-7388\(02\)00429-5](https://doi.org/10.1016/S0376-7388(02)00429-5).
- 730 [6] M.Z. Ahmad, R. Castro-Munóz, P.M. Budd, Boosting gas separation  
731 performance and suppressing the physical aging of polymers of intrinsic  
732 microporosity (PIM-1) by nanomaterial blending, *Nanoscale.* 12 (2020) 23333–  
733 23370. <https://doi.org/10.1039/d0nr07042d>.
- 734 [7] R. Castro-Muñoz, M. Zamidi Ahmad, M. Malankowska, J. Coronas, A new  
735 relevant membrane application: CO<sub>2</sub> direct air capture (DAC), *Chem. Eng. J.*  
736 446 (2022). <https://doi.org/10.1016/j.cej.2022.137047>.
- 737 [8] J. Dechnik, J. Gascon, C.J. Doonan, C. Janiak, C.J. Sumbly, Mixed-Matrix  
738 Membranes, *Angew. Chemie - Int. Ed.* 56 (2017) 9292–9310.  
739 <https://doi.org/10.1002/anie.201701109>.
- 740 [9] Y. Shi, B. Liang, R.B. Lin, C. Zhang, B. Chen, Gas Separation via Hybrid Metal–  
741 Organic Framework/Polymer Membranes, *Trends Chem.* 2 (2020) 254–269.  
742 <https://doi.org/10.1016/j.trechm.2020.01.002>.
- 743 [10] A.R. Kamble, C.M. Patel, Z.V.P. Murthy, A review on the recent advances in  
744 mixed matrix membranes for gas separation processes, *Renew. Sustain. Energy*  
745 *Rev.* 145 (2021) 111062. <https://doi.org/10.1016/j.rser.2021.111062>.
- 746 [11] R. Castro-Muñoz, A. Cruz-Cruz, Y. Alfaro-Sommers, L.X. Aranda-Jarillo, E.  
747 Gontarek-Castro, Reviewing the recent developments of using graphene-based  
748 nanosized materials in membrane separations, *Crit. Rev. Environ. Sci. Technol.*  
749 0 (2021) 1–38. <https://doi.org/10.1080/10643389.2021.1918509>.
- 750 [12] Y. Zhang, X. Feng, S. Yuan, J. Zhou, B. Wang, Challenges and recent advances  
751 in MOF-polymer composite membranes for gas separation, *Inorg. Chem. Front.*  
752 3 (2016) 896–909. <https://doi.org/10.1039/c6qi00042h>.



- 753 [13] J. Müller, K.V. Peinemann, J. Müller, Development of facilitated transport  
754 membranes for the separation of olefins from gas streams, *Desalination*. 145  
755 (2002) 339–345. [https://doi.org/10.1016/S0011-9164\(02\)00433-2](https://doi.org/10.1016/S0011-9164(02)00433-2).
- 756 [14] G. Dong, H. Li, V. Chen, Challenges and opportunities for mixed-matrix  
757 membranes for gas separation, *J. Mater. Chem. A*. 1 (2013) 4610–4630.  
758 <https://doi.org/10.1039/c3ta00927k>.
- 759 [15] Z. Lai, M. Tsapatsis, Gas and organic vapor permeation through b-oriented MFI  
760 membranes, *Ind. Eng. Chem. Res.* 43 (2004) 3000–3007.  
761 <https://doi.org/10.1021/ie034096s>.
- 762 [16] X. Zhao, Y. Wang, D.S. Li, X. Bu, P. Feng, Metal–Organic Frameworks for  
763 Separation, *Adv. Mater.* 30 (2018). <https://doi.org/10.1002/adma.201705189>.
- 764 [17] H. Li, C. Qiu, S. Ren, Q. Dong, S. Zhang, F. Zhou, X. Liang, J. Wang, S. Li, M.  
765 Yu, Na<sup>+</sup>-gated water-conducting nanochannels for boosting CO<sub>2</sub> conversion to  
766 liquid fuels, *Science* (80-. ). 367 (2020) 667–671.  
767 <https://doi.org/10.1126/science.aaz6053>.
- 768 [18] Y. Peng, Y. Li, Y. Ban, H. Jin, W. Jiao, X. Liu, W. Yang, Metal-organic framework  
769 nanosheets as building blocks for molecular sieving membranes, *Science* (80-. ).  
770 346 (2014) 1356–1359.
- 771 [19] M. Dakhchoune, L.F. Villalobos, R. Semino, L. Liu, M. Rezaei, P. Schouwink,  
772 C.E. Avalos, P. Baade, V. Wood, Y. Han, M. Ceriotti, K.V. Agrawal, Gas-sieving  
773 zeolitic membranes fabricated by condensation of precursor nanosheets, *Nat.*  
774 *Mater.* 20 (2021) 362–369. <https://doi.org/10.1038/s41563-020-00822-2>.
- 775 [20] B. Wang, T. Wu, M. Yu, S. Li, R. Zhou, W. Xing, Highly Ordered Nanochannels  
776 in a Nanosheet-Directed Thin Zeolite Nanofilm for Precise and Fast CO<sub>2</sub>  
777 Separation, *Small*. 16 (2020). <https://doi.org/10.1002/smll.202002836>.
- 778 [21] B. Wang, N. Wang, X. Li, R. Zhou, W. Xing, Exfoliation of lamellar SAPO-34  
779 zeolite to nanosheets and synthesis of thin SAPO-34 membranes by a  
780 nanosheet-seeded secondary growth approach, *J. Memb. Sci.* 645 (2022)



- 781 120177. <https://doi.org/10.1016/j.memsci.2021.120177>.
- 782 [22] J. Zhao, S.H. Mousavi, G. Xiao, A.H. Mokarizadeh, T. Moore, K. Chen, Q. Gu, R.  
783 Singh, A. Zavabeti, J.Z. Liu, P.A. Webley, G.K. Li, Nitrogen Rejection from  
784 Methane via a “Trapdoor” K-ZSM-25 Zeolite, *J. Am. Chem. Soc.* 143 (2021)  
785 15195–15204. <https://doi.org/10.1021/jacs.1c06230>.
- 786 [23] G. Liu, V. Chernikova, Y. Liu, K. Zhang, Y. Belmabkhout, O. Shekhah, C. Zhang,  
787 S. Yi, M. Eddaoudi, W.J. Koros, Mixed matrix formulations with MOF molecular  
788 sieving for key energy-intensive separations, *Nat. Mater.* 17 (2018) 283–289.  
789 <https://doi.org/10.1038/s41563-017-0013-1>.
- 790 [24] J.J. Low, A.I. Benin, P. Jakubczak, J.F. Abrahamian, S.A. Faheem, R.R. Willis,  
791 Virtual high throughput screening confirmed experimentally: Porous coordination  
792 polymer hydration, *J. Am. Chem. Soc.* 131 (2009) 15834–15842.  
793 <https://doi.org/10.1021/ja9061344>.
- 794 [25] H. Zhai, Advanced Membranes and Learning Scale Required for Cost-Effective  
795 Post-combustion Carbon Capture, *IScience.* 13 (2019) 440–451.  
796 <https://doi.org/10.1016/j.isci.2019.03.006>.
- 797 [26] N. Kosinov, V.G.P. Sripathi, E.J.M. Hensen, Improving separation performance  
798 of high-silica zeolite membranes by surface modification with  
799 triethoxyfluorosilane, *Microporous Mesoporous Mater.* 194 (2014) 24–30.  
800 <https://doi.org/10.1016/j.micromeso.2014.03.034>.
- 801 [27] X. Liu, Y. Li, Y. Ban, Y. Peng, H. Jin, H. Bux, L. Xu, W. Yang, Improvement of  
802 hydrothermal stability of zeolitic imidazolate frameworks, *Chem. Commun.* 49  
803 (2013) 9140–9142. <https://doi.org/10.1039/c3cc45308a>.
- 804 [28] M. Navarro, E. Mateo, B. Diosdado, M. Tsapatsis, J. Coronas, Activation of giant  
805 silicalite-1 monocrystals combining rapid thermal processing and ozone  
806 calcination, *RSC Adv.* 5 (2015) 18035–18040.  
807 <https://doi.org/10.1039/c4ra16284f>.
- 808 [29] L. Wang, C. Zhang, X. Gao, L. Peng, J. Jiang, X. Gu, Preparation of defect-free



- 809 DDR zeolite membranes by eliminating template with ozone at low temperature,  
810 J. Memb. Sci. 539 (2017) 152–160.  
811 <https://doi.org/10.1016/j.memsci.2017.06.004>.
- 812 [30] M.Y. Jeon, D. Kim, P. Kumar, P.S. Lee, N. Rangnekar, P. Bai, M. Shete, B.  
813 Elyassi, H.S. Lee, K. Narasimharao, S.N. Basahel, S. Al-Thabaiti, W. Xu, H.J.  
814 Cho, E.O. Fetisov, R. Thyagarajan, R.F. DeJaco, W. Fan, K.A. Mkhoyan, J.I.  
815 Siepmann, M. Tsapatsis, Ultra-selective high-flux membranes from directly  
816 synthesized zeolite nanosheets, Nature. 543 (2017) 690–694.  
817 <https://doi.org/10.1038/nature21421>.
- 818 [31] K. Varoon, X. Zhang, B. Elyassi, D.D. Brewer, M. Gettel, S. Kumar, J. Lee, S.  
819 Maheshwari, A. Mittal, C. Sung, M. Cococcioni, L. Franxis, A. McCormick, K.  
820 Mkhoyan, M. Tsapatsis, Dispersible Exfoliated Zeolite Nanosheets and Their  
821 Application as a Selective Membrane, Science (80-. ). 334 (2011) 72–75.
- 822 [32] J. Yu, Y. Pan, C. Wang, Z. Lai, ZIF-8 membranes with improved reproducibility  
823 fabricated from sputter-coated ZnO/alumina supports, Chem. Eng. Sci. 141  
824 (2016) 119–124. <https://doi.org/10.1016/j.ces.2015.10.035>.
- 825 [33] L. NGK INSULATORS, NGK's Large Ceramic Membrane to Be Used in  
826 Demonstration Test for CO<sub>2</sub> Recovery from Associated Gas during Oil  
827 Production, (2019). <https://www.ngk-insulators.com/en/>.
- 828 [34] Y. Pan, Z. Lai, Sharp separation of C<sub>2</sub>/C<sub>3</sub> hydrocarbon mixtures by zeolitic  
829 imidazolate framework-8 (ZIF-8) membranes synthesized in aqueous solutions,  
830 Chem. Commun. 47 (2011) 10275–10277. <https://doi.org/10.1039/c1cc14051e>.
- 831 [35] J. Yao, D. Dong, D. Li, L. He, G. Xu, H. Wang, Contra-diffusion synthesis of ZIF-  
832 8 films on a polymer substrate, Chem. Commun. 47 (2011) 2559–2561.  
833 <https://doi.org/10.1039/c0cc04734a>.
- 834 [36] R. Wei, H.Y. Chi, X. Li, D. Lu, Y. Wan, C.W. Yang, Z. Lai, Aqueously Cathodic  
835 Deposition of ZIF-8 Membranes for Superior Propylene/Propane Separation,  
836 Adv. Funct. Mater. 30 (2020) 1–7. <https://doi.org/10.1002/adfm.201907089>.



- 837 [37] G. He, M. Dakhchoune, J. Zhao, S. Huang, K.V. Agrawal, Electrophoretic Nuclei  
838 Assembly for Crystallization of High-Performance Membranes on Unmodified  
839 Supports, *Adv. Funct. Mater.* 28 (2018) 1–8.  
840 <https://doi.org/10.1002/adfm.201707427>.
- 841 [38] S. Zhou, Y. Wei, L. Li, Y. Duan, Q. Hou, L. Zhang, L.X. Ding, J. Xue, H. Wang, J.  
842 Caro, Paralyzed membrane: Current-driven synthesis of a metal-organic  
843 framework with sharpened propene/propane separation, *Sci. Adv.* 4 (2018) 1–8.  
844 <https://doi.org/10.1126/sciadv.aau1393>.
- 845 [39] I.G. Wenten, P.T. Dharmawijaya, P.T.P. Aryanti, R.R. Mukti, Khoiruddin, LTA  
846 zeolite membranes: Current progress and challenges in pervaporation, *RSC*  
847 *Adv.* 7 (2017) 29520–29539. <https://doi.org/10.1039/c7ra03341a>.
- 848 [40] A.W. Thornton, B.D. Freeman, L.M. Robeson, Polymer Gas Separation  
849 Membrane Database, (2012).  
850 [https://research.csiro.au/virtualsecreening/membrane-database-polymer-gas-](https://research.csiro.au/virtualsecreening/membrane-database-polymer-gas-separation-membranes/)  
851 [separation-membranes/](https://research.csiro.au/virtualsecreening/membrane-database-polymer-gas-separation-membranes/).
- 852 [41] M.R. Abdul Hamid, Y. Qian, R. Wei, Z. Li, Y. Pan, Z. Lai, H.K. Jeong,  
853 Polycrystalline metal-organic framework (MOF) membranes for molecular  
854 separations: Engineering prospects and challenges, *J. Memb. Sci.* 640 (2021)  
855 119802. <https://doi.org/10.1016/j.memsci.2021.119802>.
- 856 [42] T. Rodenas, I. Luz, G. Prieto, B. Seoane, H. Miro, A. Corma, F. Kapteijn, F.  
857 Xamena, J. Gascon, Metal–organic framework nanosheets in polymer composite  
858 materials for gas separation, *Nat. Mater.* 14 (2015) 48–55.
- 859 [43] L.F. Villalobos, M.T. Vahdat, M. Dakhchoune, Z. Nadizadeh, M. Mensi, E.  
860 Oveisi, D. Campi, N. Marzari, K.V. Agrawal, Large-scale synthesis of crystalline  
861 g-C<sub>3</sub>N<sub>4</sub> nanosheets and high-temperature H<sub>2</sub> sieving from assembled films, *Sci.*  
862 *Adv.* 6 (2020) 1–9. <https://doi.org/10.1126/sciadv.aay9851>.
- 863 [44] Z. Kang, Y. Peng, Y. Qian, D. Yuan, M.A. Addicoat, T. Heine, Z. Hu, L. Tee, Z.  
864 Guo, D. Zhao, Mixed Matrix Membranes (MMMs) Comprising Exfoliated 2D



- 865 Covalent Organic Frameworks (COFs) for Efficient CO<sub>2</sub> Separation, *Chem.*  
866 *Mater.* 28 (2016) 1277–1285. <https://doi.org/10.1021/acs.chemmater.5b02902>.
- 867 [45] H.W. Kim, E. Al., Selective Gas Transport Through Few-Layered Graphene and  
868 Graphene Oxide Membranes, *Science* (80-. ). 342 (2014) 91–95.  
869 <https://doi.org/10.1126/science.1236098>.
- 870 [46] X. Sang, Y. Xie, D.E. Yilmaz, R. Lotfi, M. Alhabeab, A. Ostadhossein, B. Anasori,  
871 W. Sun, X. Li, K. Xiao, P.R.C. Kent, A.C.T. Van Duin, Y. Gogotsi, R.R. Unocic, In  
872 situ atomistic insight into the growth mechanisms of single layer 2D transition  
873 metal carbides, *Nat. Commun.* 9 (2018) 1–9. [https://doi.org/10.1038/s41467-](https://doi.org/10.1038/s41467-018-04610-0)  
874 [018-04610-0](https://doi.org/10.1038/s41467-018-04610-0).
- 875 [47] J. Shen, G. Liu, K. Huang, W. Jin, K.-R. Lee, N. Xu, Membranes with Fast and  
876 Selective Gas-Transport Channels of Laminar Graphene Oxide for Efficient CO  
877 2 Capture , *Angew. Chemie.* 127 (2015) 588–592.  
878 <https://doi.org/10.1002/ange.201409563>.
- 879 [48] J. Abraham, K.S. Vasu, C.D. Williams, K. Gopinadhan, Y. Su, C.T. Cherian, J.  
880 Dix, E. Prestat, S.J. Haigh, I. V Grigorieva, P. Carbone, A.K. Geim, R.R. Nair,  
881 Tunable sieving of ions using graphene oxide membranes, *Nat. Nanotechnol.*  
882 (2017) 1–6. <https://doi.org/10.1038/nnano.2017.21>.
- 883 [49] R. Castro-Muñoz, J. Buera-González, Ó. de la Iglesia, F. Galiano, V. Fíla, M.  
884 Malankowska, C. Rubio, A. Figoli, C. Téllez, J. Coronas, Towards the  
885 dehydration of ethanol using pervaporation cross-linked poly(vinyl  
886 alcohol)/graphene oxide membranes, *J. Memb. Sci.* 582 (2019) 423–434.  
887 <https://doi.org/10.1016/j.memsci.2019.03.076>.
- 888 [50] K. Celebi, J. Buchheim, R.M. Wyss, A. Droudian, P. Gasser, I. Shorubalko, J.-I.  
889 Kye, C. Lee, H.G. Park, Ultimate Permeation Across Atomically Thin Porous  
890 Graphene, *Science* (80-. ). 344 (2014) 289–292.  
891 <https://doi.org/10.1126/science.1249097>.
- 892 [51] C. Sun, B. Wen, B. Bai, Application of nanoporous graphene membranes in



- 893 natural gas processing: Molecular simulations of CH<sub>4</sub>/CO<sub>2</sub>, CH<sub>4</sub>/H<sub>2</sub>S and  
894 CH<sub>4</sub>/N<sub>2</sub> separation, *Chem. Eng. Sci.* 138 (2015) 616–621.  
895 <https://doi.org/10.1016/j.ces.2015.08.049>.
- 896 [52] S. Huang, S. Li, L.F. Villalobos, M. Dakhchoune, M. Micari, D.J. Babu, M.T.  
897 Vahdat, M. Mensi, E. Oveisi, K.V. Agrawal, Millisecond lattice gasification for  
898 high-density CO<sub>2</sub>- And O<sub>2</sub>-sieving nanopores in single-layer graphene, *Sci. Adv.*  
899 7 (2021) 1–13. <https://doi.org/10.1126/sciadv.abf0116>.
- 900 [53] S.P. Koenig, L. Wang, J. Pellegrino, J.S. Bunch, Selective molecular sieving  
901 through porous graphene, *Nat. Nanotechnol.* 7 (2012) 728–732.
- 902 [54] Z. Yuan, A. Govind Rajan, R.P. Misra, L.W. Drahushuk, K.V. Agrawal, M.S.  
903 Strano, D. Blankschtein, Mechanism and Prediction of Gas Permeation through  
904 Sub-Nanometer Graphene Pores: Comparison of Theory and Simulation, *ACS*  
905 *Nano.* 11 (2017) 7974–7987. <https://doi.org/10.1021/acsnano.7b02523>.
- 906 [55] N. Li, Y. Tian, J. Zhang, Z. Sun, J. Zhao, J. Zhang, W. Zuo, Precisely-controlled  
907 modification of PVDF membranes with 3D TiO<sub>2</sub> / ZnO nanolayer : enhanced  
908 anti-fouling performance by changing hydrophilicity and photocatalysis under  
909 visible light irradiation, *J. Memb. Sci.* 528 (2017) 359–368.  
910 <https://doi.org/10.1016/j.memsci.2017.01.048>.
- 911 [56] B. Luan, B. Elmegreen, M.A. Kuroda, Z. Gu, G. Lin, S. Zeng, Crown Nanopores  
912 in Graphene for CO<sub>2</sub> Capture and Filtration, *ACS Nano.* (2022).  
913 <https://doi.org/10.1021/acsnano.2c00213>.
- 914 [57] K.J. Hsu, L.F. Villalobos, S. Huang, H.Y. Chi, M. Dakhchoune, W.C. Lee, G. He,  
915 M. Mensi, K.V. Agrawal, Multipulsed Millisecond Ozone Gasification for  
916 Predictable Tuning of Nucleation and Nucleation-Decoupled Nanopore  
917 Expansion in Graphene for Carbon Capture, *ACS Nano.* 15 (2021) 13230–  
918 13239. <https://doi.org/10.1021/acsnano.1c02927>.
- 919 [58] H. Zhang, Q. Xiao, X. Guo, N. Li, P. Kumar, N. Rangnekar, Y. Jeon, S. Al-  
920 thabaiti, K. Narasimharao, S.N. Basahel, B. Topuz, F.J. Onorato, C.W. Macosko,





- 921 K.A. Mkhoyan, M. Tsapatsis, Open-Pore Two-Dimensional MFI Zeolite  
922 Nanosheets for the Fabrication of Hydrocarbon-Isomer-Selective Membranes  
923 on Porous Polymer Supports, *Angew. Chemie - Int. Ed.* 300072 (2016) 7184–  
924 7187. <https://doi.org/10.1002/anie.201601135>.
- 925 [59] P.R. Kidambi, D.D. Mariappan, N.T. Dee, A. Vyatskikh, S. Zhang, R. Karnik, A.J.  
926 Hart, A Scalable Route to Nanoporous Large-Area Atomically Thin Graphene  
927 Membranes by Roll-to-Roll Chemical Vapor Deposition and Polymer Support  
928 Casting, *ACS Appl. Mater. Interfaces.* 10 (2018) 10369–10378.  
929 <https://doi.org/10.1021/acsami.8b00846>.
- 930 [60] Y.P. Hsieh, C.H. Shih, Y.J. Chiu, M. Hofmann, High-Throughput Graphene  
931 Synthesis in Gapless Stacks, *Chem. Mater.* 28 (2016) 40–43.  
932 <https://doi.org/10.1021/acs.chemmater.5b04007>.
- 933 [61] Z. Yuan, G. He, S. Faucher, M. Kuehne, S.X. Li, D. Blankschtein, M.S. Strano,  
934 Direct Chemical Vapor Deposition Synthesis of Porous Single-Layer Graphene  
935 Membranes with High Gas Permeances and Selectivities, *Adv. Mater.* 33 (2021).  
936 <https://doi.org/10.1002/adma.202104308>.
- 937 [62] P.R. Kidambi, G.D. Nguyen, S. Zhang, Q. Chen, J. Kong, J. Warner, A.P. Li, R.  
938 Karnik, Facile Fabrication of Large-Area Atomically Thin Membranes by Direct  
939 Synthesis of Graphene with Nanoscale Porosity, *Adv. Mater.* 30 (2018).  
940 <https://doi.org/10.1002/adma.201804977>.
- 941 [63] L.F. Villalobos, C. Van Goethem, K.J. Hsu, S. Li, M. Moradi, K. Zhao, M.  
942 Dakhchoune, S. Huang, Y. Shen, E. Oveisi, V. Boureau, K.V. Agrawal, Bottom-  
943 up synthesis of graphene films hosting atom-thick molecular-sieving apertures,  
944 *Proc. Natl. Acad. Sci. U. S. A.* 118 (2021) 1–10.  
945 <https://doi.org/10.1073/pnas.2022201118>.
- 946 [64] W.C. Lee, L. Bondaz, S. Huang, G. He, M. Dakhchoune, K.V. Agrawal,  
947 Centimeter-scale gas-sieving nanoporous single-layer graphene membrane, *J.*  
948 *Memb. Sci.* 618 (2021) 118745. <https://doi.org/10.1016/j.memsci.2020.118745>.

- 949 [65] Y. Yang, X. Yang, L. Liang, Y. Gao, H. Cheng, X. Li, M. Zou, A. Cao, R. Ma, Q.  
950 Yuan, X. Duan, Large-area graphene-nanomesh/carbon-nanotube hybrid  
951 membranes for ionic and molecular nanofiltration, *Science* (80-. ). 1062 (2019)  
952 1057–1062.
- 953 [66] H. Wu, J. Thibault, B. Kruczek, The validity of the time-lag method for the  
954 characterization of mixed-matrix membranes, *J. Memb. Sci.* 618 (2021) 118715.  
955 <https://doi.org/10.1016/j.memsci.2020.118715>.
- 956 [67] R. Selyanchyn, M. Ariyoshi, S. Fujikawa, Thickness Effect on CO<sub>2</sub>/N<sub>2</sub>  
957 Separation in Double Layer Pebax-1657®/PDMS Membranes, *Membranes*  
958 (Basel). 8 (2018). <https://doi.org/10.3390/membranes8040121>.
- 959 [68] M. Kattula, K. Ponnuru, L. Zhu, W. Jia, H. Lin, E.P. Furlani, Designing ultrathin  
960 film composite membranes: The impact of a gutter layer, *Sci. Rep.* 5 (2015) 1–9.  
961 <https://doi.org/10.1038/srep15016>.
- 962 [69] M. Jin Yoo, K. Hyun, J. Hyeok, T. Woo, C. Wook, Ultrathin gutter layer for high-  
963 performance thin- fi lm composite membranes for CO<sub>2</sub> separation, *J. Memb.*  
964 *Sci.* 566 (2018) 336–345. <https://doi.org/10.1016/j.memsci.2018.09.017>.
- 965 [70] L. Martínez-Izquierdo, M. Malankowska, J. Sánchez-Lainez, C. Téllez, J.  
966 Coronas, Poly(ether-block-amide) copolymer membrane for CO<sub>2</sub>/N<sub>2</sub> separation:  
967 The influence of the casting solution concentration on its morphology, thermal  
968 properties and gas separation performance, *R. Soc. Open Sci.* 6 (2019).  
969 <https://doi.org/10.1098/rsos.190866>.
- 970 [71] V.I. Bondar, B.D. Freeman, I. Pinnau, Gas Transport Properties of Poly ( ether-  
971 b-amide ) Segmented, *J. Polym. Sci. Part B Polym. Physics*,. 38 (2000) 2051–  
972 2062.
- 973 [72] Y. Wang, H. Li, G. Dong, C. Scholes, V. Chen, Effect of Fabrication and  
974 Operation Conditions on CO<sub>2</sub> Separation Performance of PEO-PA Block  
975 Copolymer Membranes, *Ind. Eng. Chem. Res.* 54 (2015) 7273–7283.  
976 <https://doi.org/10.1021/acs.iecr.5b01234>.



- 977 [73] J.H. Kim, S.Y. Ha, Y.M. Lee, Gas permeation of poly(amide-6-b-ethylene oxide)  
978 copolymer, *J. Memb. Sci.* 190 (2001) 179–193. [https://doi.org/10.1016/S0376-](https://doi.org/10.1016/S0376-7388(01)00444-6)  
979 7388(01)00444-6.
- 980 [74] V. Mozaffari, M. Sadeghi, A. Fakhar, G. Khanbabaei, A.F. Ismail, Gas separation  
981 properties of polyurethane/poly(ether-block-amide) (PU/PEBA) blend  
982 membranes, *Sep. Purif. Technol.* 185 (2017) 202–214.  
983 <https://doi.org/10.1016/j.seppur.2017.05.028>.
- 984 [75] R.S. Murali, S. Sridhar, T. Sankarshana, Y.V.L. Ravikumar, Gas Permeation  
985 Behavior of Pebax-1657 Nanocomposite Membrane Incorporated with  
986 Multiwalled Carbon Nanotubes, *Ind. Eng. Chem. Res.* 49 (2010) 6530–6538.  
987 <https://doi.org/10.1021/ie9016495>.
- 988 [76] B. Yu, H. Cong, Z. Li, J. Tang, X.S. Zhao, Pebax-1657 nanocomposite  
989 membranes incorporated with nanoparticles/ colloids/carbon nanotubes for  
990 CO<sub>2</sub>/N<sub>2</sub> and CO<sub>2</sub>/H<sub>2</sub> separation, *J. Appl. Polym. Sci.* 130 (2013) 2867–2876.  
991 <https://doi.org/10.1002/app.39500>.
- 992 [77] D. Zhao, J. Ren, H. Li, X. Li, M. Deng, Gas separation properties of poly(amide-  
993 6-b-ethylene oxide)/amino modified multi-walled carbon nanotubes mixed matrix  
994 membranes, *J. Memb. Sci.* 467 (2014) 41–47.  
995 <https://doi.org/10.1016/j.memsci.2014.05.009>.
- 996 [78] S.D. Bazhenov, I.L. Borisov, D.S. Bakhtin, A.N. Rybakova, V.S. Khotimskiy, S.P.  
997 Molchanov, V. V. Volkov, High-permeance crosslinked PTMSP thin-film  
998 composite membranes as supports for CO<sub>2</sub> selective layer formation, *Green*  
999 *Energy Environ.* 1 (2016) 235–245. <https://doi.org/10.1016/j.gee.2016.10.002>.
- 1000 [79] S. Fujikawa, M. Ariyoshi, R. Selyanchyn, T. Kunitake, Ultra-fast, selective CO<sub>2</sub>  
1001 permeation by free-standing siloxane nanomembranes, *Chem. Lett.* 48 (2019)  
1002 1351–1354. <https://doi.org/10.1246/cl.190558>.
- 1003 [80] B. Seoane, A. Dikhtiarenko, A. Mayoral, C. Tellez, J. Coronas, F. Kapteijn, J.  
1004 Gascon, Metal organic framework synthesis in the presence of surfactants:



- 1005 Towards hierarchical MOFs?, *CrystEngComm*. 17 (2015) 1693–1700.  
1006 <https://doi.org/10.1039/c4ce02324b>.
- 1007 [81] O. Selyanchyn, R. Selyanchyn, S. Fujikawa, Critical Role of the Molecular  
1008 Interface in Double-Layered Pebax-1657/PDMS Nanomembranes for Highly  
1009 Efficient CO<sub>2</sub>/N<sub>2</sub> Gas Separation, *ACS Appl. Mater. Interfaces*. 12 (2020)  
1010 33196–33209. <https://doi.org/10.1021/acsami.0c07344>.
- 1011 [82] A. Car, C. Stropnik, W. Yave, K. Peinemann, Pebax® / polyethylene glycol  
1012 blend thin film composite membranes for CO<sub>2</sub> separation : Performance with  
1013 mixed gases, *Sep. Purif. Technol.* 62 (2008) 110–117.  
1014 <https://doi.org/10.1016/j.seppur.2008.01.001>.
- 1015 [83] L. Wang, Y. Li, S. Li, P. Ji, C. Jiang, Preparation of composite poly(ether block  
1016 amide) membrane for CO<sub>2</sub> capture, *J. Energy Chem.* 23 (2014) 717–725.  
1017 [https://doi.org/10.1016/S2095-4956\(14\)60204-7](https://doi.org/10.1016/S2095-4956(14)60204-7).
- 1018 [84] X. Ren, J. Ren, H. Li, S. Feng, M. Deng, Poly (amide-6-b-ethylene oxide)  
1019 multilayer composite membrane for carbon dioxide separation, *Int. J. Greenh.*  
1020 *Gas Control.* 8 (2012) 111–120. <https://doi.org/10.1016/j.ijggc.2012.01.017>.
- 1021 [85] T. Li, Y. Pan, K.V. Peinemann, Z. Lai, Carbon dioxide selective mixed matrix  
1022 composite membrane containing ZIF-7 nano-fillers, *J. Memb. Sci.* 425–426  
1023 (2013) 235–242. <https://doi.org/10.1016/j.memsci.2012.09.006>.
- 1024 [86] P.D. Sutrisna, J. Hou, H. Li, Y. Zhang, V. Chen, Improved operational stability of  
1025 Pebax-based gas separation membranes with ZIF-8: A comparative study of flat  
1026 sheet and composite hollow fibre membranes, *J. Memb. Sci.* 524 (2017) 266–  
1027 279. <https://doi.org/10.1016/j.memsci.2016.11.048>.
- 1028 [87] P.D. Sutrisna, J. Hou, M.Y. Zulkifli, H. Li, Y. Zhang, W. Liang, D.M.  
1029 D'Alessandro, V. Chen, Surface functionalized UiO-66/Pebax-based ultrathin  
1030 composite hollow fiber gas separation membranes, *J. Mater. Chem. A*. 6 (2018)  
1031 918–931. <https://doi.org/10.1039/c7ta07512j>.
- 1032 [88] J. Kim, Q. Fu, K. Xie, J.M.P. Scofield, S.E. Kentish, G.G. Qiao, CO<sub>2</sub> separation



- 1033 using surface-functionalized SiO<sub>2</sub> nanoparticles incorporated ultra-thin film  
1034 composite mixed matrix membranes for post-combustion carbon capture, *J.*  
1035 *Memb. Sci.* 515 (2016) 54–62. <https://doi.org/10.1016/j.memsci.2016.05.029>.
- 1036 [89] S. Karan, Z. Jiang, A. Livingston, Sub-10 nm polyamide nanofilms with ultrafast  
1037 solvent transport for molecular separation, *Science* (80-. ). 348 (2015) 1347–  
1038 1351.
- 1039 [90] T.C. Merkel, H. Lin, X. Wei, R. Baker, Power plant post-combustion carbon  
1040 dioxide capture: An opportunity for membranes, *J. Memb. Sci.* 359 (2010) 126–  
1041 139. <https://doi.org/10.1016/j.memsci.2009.10.041>.
- 1042 [91] L.S. White, K.D. Amo, T. Wu, T.C. Merkel, Extended field trials of Polaris sweep  
1043 modules for carbon capture, *J. Memb. Sci.* 542 (2017) 217–225.  
1044 <https://doi.org/https://doi.org/10.1016/j.memsci.2017.08.017>.
- 1045 [92] M. Etxeberria-Benavides, T. Johnson, S. Cao, B. Zornoza, J. Coronas, J.  
1046 Sanchez-Lainez, A. Sabetghadam, X. Liu, E. Andres-Garcia, F. Kapteijn, J.  
1047 Gascon, O. David, PBI mixed matrix hollow fiber membrane: Influence of ZIF-8  
1048 filler over H<sub>2</sub>/CO<sub>2</sub> separation performance at high temperature and pressure,  
1049 *Sep. Purif. Technol.* 237 (2020) 116347.  
1050 <https://doi.org/10.1016/j.seppur.2019.116347>.
- 1051 [93] Y. Zhang, Q. Shen, J. Hou, P. Sutrisna, V. Chen, Shear-aligned graphene oxide  
1052 laminate/Pebax ultrathin composite hollow fiber membranes using a facile dip-  
1053 coating approach, *J. Mater. Chem. A* 5 (2017) 7732–7737.  
1054 <https://doi.org/10.1039/c6ta10395b>.
- 1055 [94] M. Mohammadi Ghaleni, M. Bavarian, S. Nejati, Model-guided design of high-  
1056 performance membrane distillation modules for water desalination, *J. Memb.*  
1057 *Sci.* 563 (2018) 794–803. <https://doi.org/10.1016/j.memsci.2018.06.054>.
- 1058 [95] R.W. Baker, Future Directions of Membrane Gas Separation Technology, *Ind.*  
1059 *Eng. Chem. Res.* 41 (2002) 1393–1411. <https://doi.org/10.1021/ie0108088>.
- 1060 [96] Y. Ding, Perspective on Gas Separation Membrane Materials from Process



- 1061 Economics Point of View, *Ind. Eng. Chem. Res.* 59 (2020) 556–568.  
1062 <https://doi.org/10.1021/acs.iecr.9b05975>.
- 1063 [97] E. Akhondi, F. Zamani, K.H. Tng, G. Leslie, W.B. Krantz, A.G. Fane, J.W. Chew,  
1064 The performance and fouling control of submerged hollow fiber (HF) systems: A  
1065 review, *Appl. Sci.* 7 (2017) 1–39. <https://doi.org/10.3390/app7080765>.
- 1066 [98] K.K. Chen, W. Salim, Y. Han, D. Wu, W.S.W. Ho, Fabrication and scale-up of  
1067 multi-leaf spiral-wound membrane modules for CO<sub>2</sub> capture from flue gas, *J.*  
1068 *Memb. Sci.* 595 (2020) 117504. <https://doi.org/10.1016/j.memsci.2019.117504>.
- 1069 [99] Y. Han, W. Salim, K.K. Chen, D. Wu, W.S.W. Ho, Field trial of spiral-wound  
1070 facilitated transport membrane module for CO<sub>2</sub> capture from flue gas, *J. Memb.*  
1071 *Sci.* 575 (2019) 242–251. <https://doi.org/10.1016/j.memsci.2019.01.024>.
- 1072 [100] W. Salim, V. Vakharia, Y. Chen, D. Wu, Y. Han, W.S.W. Ho, Fabrication and  
1073 field testing of spiral-wound membrane modules for CO<sub>2</sub> capture from flue gas,  
1074 *J. Memb. Sci.* 556 (2018) 126–137.  
1075 <https://doi.org/10.1016/j.memsci.2018.04.001>.
- 1076 [101] R. Castro-Muñoz, K.V. Agrawal, J. Coronas, Ultrathin permselective  
1077 membranes: the latent way for efficient gas separation, *RSC Adv.* 10 (2020)  
1078 12653–12670. <https://doi.org/10.1039/d0ra02254c>.
- 1079 [102] L. Wang, M.S.H. Boutilier, P.R. Kidambi, D. Jang, N.G. Hadjiconstantinou, R.  
1080 Karnik, Fundamental transport mechanisms, fabrication and potential  
1081 applications of nanoporous atomically thin membranes, *Nat. Nanotechnol.* 12  
1082 (2017) 509–522. <https://doi.org/10.1038/nnano.2017.72>.
- 1083 [103] R.W. Baker, B.T. Low, Gas Separation Membrane Materials: A Perspective,  
1084 *Macromolecules.* 47 (2014) 6999–7013.
- 1085 [104] Y. Dai, J.R. Johnson, O. Karvan, D.S. Sholl, W.J. Koros, Ultem®/ZIF-8 mixed  
1086 matrix hollow fiber membranes for CO<sub>2</sub>/N<sub>2</sub> separations, *J. Memb. Sci.* 401–402  
1087 (2012) 76–82. <https://doi.org/10.1016/j.memsci.2012.01.044>.
- 1088 [105] W.F. Yong, T.S. Chung, M. Weber, C. Maletzko, New polyethersulfone (PESU)



- 1089 hollow fiber membranes for CO<sub>2</sub> capture, *J. Memb. Sci.* 552 (2018) 305–314.  
1090 <https://doi.org/10.1016/j.memsci.2018.02.008>.
- 1091 [106] J. Sánchez-Laínez, M. Etxeberria-Benavides, O. David, C. Téllez, J. Coronas,  
1092 Green Preparation of Thin Films of Polybenzimidazole on Flat and Hollow Fiber  
1093 Supports: Application to Hydrogen Separation, *ChemSusChem*. 14 (2021) 952–  
1094 960. <https://doi.org/10.1002/cssc.202002700>.
- 1095 [107] H.Z. Chen, Z. Thong, P. Li, T.S. Chung, High performance composite hollow  
1096 fiber membranes for CO<sub>2</sub>/H<sub>2</sub> and CO<sub>2</sub>/N<sub>2</sub> separation, *Int. J. Hydrogen Energy*.  
1097 39 (2014) 5043–5053. <https://doi.org/10.1016/j.ijhydene.2014.01.047>.
- 1098 [108] Z. Dai, J. Deng, L. Ansaloni, S. Janakiram, L. Deng, Thin-film-composite hollow  
1099 fiber membranes containing amino acid salts as mobile carriers for CO<sub>2</sub>  
1100 separation, *J. Memb. Sci.* 578 (2019) 61–68.  
1101 <https://doi.org/10.1016/j.memsci.2019.02.023>.
- 1102 [109] C.Z. Liang, W.F. Yong, T.S. Chung, High-performance composite hollow fiber  
1103 membrane for flue gas and air separations, *J. Memb. Sci.* 541 (2017) 367–377.  
1104 <https://doi.org/10.1016/j.memsci.2017.07.014>.
- 1105 [110] A. Naderi, T.S. Chung, M. Weber, C. Maletzko, High performance dual-layer  
1106 hollow fiber membrane of sulfonated polyphenylsulfone/Polybenzimidazole for  
1107 hydrogen purification, *J. Memb. Sci.* 591 (2019) 117292.  
1108 <https://doi.org/10.1016/j.memsci.2019.117292>.
- 1109 [111] A.K. Zulhairun, M.N. Subramaniam, A. Samavati, M.K.N. Ramli, M. Krishparao,  
1110 P.S. Goh, A.F. Ismail, High-flux polysulfone mixed matrix hollow fiber membrane  
1111 incorporating mesoporous titania nanotubes for gas separation, *Sep. Purif.*  
1112 *Technol.* 180 (2017) 13–22. <https://doi.org/10.1016/j.seppur.2017.02.039>.
- 1113 [112] J.W. Wang, N.X. Li, Z.R. Li, J.R. Wang, X. Xu, C.S. Chen, Preparation and gas  
1114 separation properties of Zeolitic imidazolate frameworks-8 (ZIF-8) membranes  
1115 supported on silicon nitride ceramic hollow fibers, *Ceram. Int.* 42 (2016) 8949–  
1116 8954. <https://doi.org/10.1016/j.ceramint.2016.02.153>.



- 1117 [113] A.K. Zulhairun, Z.G. Fachrurrazi, M. Nur Izwanne, A.F. Ismail, Asymmetric  
1118 hollow fiber membrane coated with polydimethylsiloxane-metal organic  
1119 framework hybrid layer for gas separation, *Sep. Purif. Technol.* 146 (2015) 85–  
1120 93. <https://doi.org/10.1016/j.seppur.2015.03.033>.
- 1121 [114] H. Zhu, X. Jie, Y. Cao, Fabrication of Functionalized MOFs Incorporated Mixed  
1122 Matrix Hollow Fiber Membrane for Gas Separation, *J. Chem.* 2017 (2017).  
1123 <https://doi.org/10.1155/2017/2548957>.
- 1124 [115] C.Z. Liang, J.T. Liu, J.Y. Lai, T.S. Chung, High-performance multiple-layer PIM  
1125 composite hollow fiber membranes for gas separation, *J. Memb. Sci.* 563 (2018)  
1126 93–106. <https://doi.org/10.1016/j.memsci.2018.05.045>.
- 1127 [116] G. Li, W. Kujawski, K. Knozowska, J. Kujawa, Thin Film Mixed Matrix Hollow  
1128 Fiber Membrane Fabricated by Incorporation of Amine Functionalized Metal-  
1129 Organic Framework for CO<sub>2</sub>/N<sub>2</sub> Separation, *Materials (Basel)*. 14 (2021) 3366.  
1130 <https://doi.org/10.3390/ma14123366>.
- 1131 [117] J. Yuan, H. Zhu, J. Sun, Y. Mao, G. Liu, W. Jin, Novel ZIF-300 Mixed-Matrix  
1132 Membranes for Efficient CO<sub>2</sub> Capture, *ACS Appl. Mater. Interfaces*. 9 (2017)  
1133 38575–38583. <https://doi.org/10.1021/acsami.7b12507>.
- 1134 [118] G. Li, W. Kujawski, R. Válek, S. Koter, A review - The development of hollow  
1135 fibre membranes for gas separation processes, *Int. J. Greenh. Gas Control*. 104  
1136 (2021). <https://doi.org/10.1016/j.ijggc.2020.103195>.
- 1137 [119] C.Z. Liang, W.F. Yong, T. Chung, High-performance composite hollow fi ber  
1138 membrane for fl ue gas and air separations, *J. Memb. Sci.* 541 (2017) 367–377.  
1139 <https://doi.org/10.1016/j.memsci.2017.07.014>.
- 1140 [120] C.A. Scholes, G.W. Stevens, S.E. Kentish, The effect of hydrogen sulfide ,  
1141 carbon monoxide and water on the performance of a PDMS membrane in  
1142 carbon dioxide / nitrogen separation, *J. Memb. Sci.* 350 (2010) 189–199.  
1143 <https://doi.org/10.1016/j.memsci.2009.12.027>.  
1144

